Response to Editor:

Dear ACP Editor Dr. Frank Dentener,

We would like to thank the two referees for their helpful comments, which have been fully taken into account upon manuscript revision. A point-by-point response to all the comments and a change-tracked revised version are shown below.

Best Regards,
Ying Chen

Response to comments of referee #1

General comments

Chen et al. describe the use of a numerical framework for emulation and sensitivity analysis of a regional air quality model in the development of air quality mitigation strategies for the megacity Delhi. They find that a combination of reduction in traffic emissions within the city, combined with simultaneous reductions in all emission sources in the surrounding region would lead to a reduction of PM2.5, while avoiding an increase in ozone. The reduction of traffic emissions from Delhi alone would increase peak ozone in Delhi due to the high emissions of NOx from traffic, with the resultant reduction in ozone due to changes in the O3-NOx titration effect.

These results are certainly plausible, and consistent with previous work. The potential for ozone to increase when high local NOx emissions are decreased has been well understood for decades, as has the transboundary nature of ozone and the corresponding need to control precursor emissions over large spatial scales in order to achieve reductions in ozone. The authors themselves also cite previous work showing that a large fraction of the PM2.5 in Delhi originates outside of the city. I would generally regard the results presented by Chen et al. as unremarkable, and not of sufficient scientific novelty to warrant publication in Atmospheric Chemistry and Physics. The most novel aspect of the study as I see it is the use of a statistical model emulator, combined with a technique called "global sensitivity analysis" to rapidly discover and evaluate effective emission mitigation options with a minimal amount of computational expense. The paper would potentially have merit if it had more of a technical focus on the methodology. Unfortunately, the methods are not described or evaluated well enough in the present version of the manuscript for me to be able to recommend publication. In order to be recommendable for publication, the manuscript needs major revisions focusing on better description and evaluation of the methods for model emulation and sensitivity analysis. I give suggestions for improving the manuscript in my specific comments, below.

Many thanks to the reviewer for the comments and suggestions.

The chemical relationship between O_3 and NOx has been well understood for decades, however, the reduction of O_3 pollution is still a troublesome issue for mitigation strategy. For example, recently in China, increase of O_3 is attracting increasing concern from the Chinese government

and public, despite considerable achievements in controlling $PM_{2.5}$ pollution, as described in the introduction. Only a handful of studies foresee the potential of O_3 increase in Delhi under the current mitigation strategy focusing on $PM_{2.5}$ and provide solutions for it. This work provides a quantified map for mitigating $PM_{2.5}$ pollution and tackling O_3 increase for Delhi, to avoid the O_3 side-effect that China is now facing. Our results could greatly benefit air pollution mitigation with respect to both $PM_{2.5}$ and O_3 in Delhi. In addition, as the reviewer mentioned, this work demonstrates a combined approach with WRF-Chem and statistical methods to rapidly discover and evaluate effective emission mitigation options.

We agree with the reviewer that more details regarding the methodology can improve this work. We have therefore improved the manuscript accordingly. Please find point-by-point responses below.

Specific comments:

The introduction is concise and well written, but since the novelty of the paper is in its methodological advances, it needs an expanded discussion of model emulation and global sensitivity analysis.

Thanks for the comments and suggestions. We have improved the manuscript by adding a clearer introduction to these approaches.

1) Line 134: WRF-Chem is an online model, which is capable of calculating its own meteorology. Please describe how the model is "driven" by the ECMWF meteorological data. Are they used as boundary conditions? Is some kind of nudging or data assimilation used?

We have added more description about how the model is driven by ECMWF meteorological data, as shown below.

"The ECMWF reanalysis dataset (ERA-Interim) assimilates observations with a number of nearly 10^7 per day (Dee et al., 2011), and is used for grid nudging, initial and boundary conditions for WRF-Chem with horizontal and temporal resolutions of $0.75^o \times 0.75^o$ and 6 hours, respectively."

2) Line 181: The reference given here (Iooss and Lemaitre, 2015) appears to use "global sensitivity analysis" as an umbrella term to describe a range of techniques. The authors should be more specific about what kind of global sensitivity analysis they describe in this manuscript.

The reviewer is right that there are many different ways to perform global sensitivity analysis, such as brute force, Sobol method, Fourier Amplitude Sensitivity Test (FAST), random-based-design FAST and extended FAST (eFAST). The sections 1.1 and 2.2 of a recent open-accessible work (Ryan et al., 2018) introduce and summarize well the application and theories/equations of different methods for global sensitivity analysis. In this study, we use the eFAST method to perform global sensitivity analysis. The eFAST method, first developed by Saltelli et al. (1999), is more efficient than the other method mentioned above and has been widely used in diverse areas of science (Carslaw et al., 2013;Koehler and Owen, 1996;Queipo et al., 2005;Vanuytrecht and Willems, 2014;vu et al., 2015).

We have rewritten the section 2.3 of our manuscript, added the description and equation for calculating global sensitivity indices, and provided more details about eFAST method for perform the sensitivity indices calculation. Detailed modification of section 2.3 will be shown in the point-4, combining with the responses to the points 2-4.

3) Line 185: The paper by Saltelli et al. (1999) is behind a paywall. Simply giving a reference to this study is not enough to describe the method they employ. The authors must also give a summary of how this works and how it is specifically employed in their study.

In this study, we use the eFAST method to perform global sensitivity analysis (GSA). The eFAST method, first developed by Saltelli et al. (1999), is more efficient than the other methods mentioned above and has been widely used in diverse areas of science, as stated above.

A detailed introduction to the theory and equations of the eFAST method is given in an open-accessible methodological study (Ryan et al., 2018). We have extensively modified section 2.3 of our manuscript to provide a simple introduction to the approaches adopted, and refer to Ryan et al. (2018) and other previous studies for further details.

Description of global sensitivity analysis in the section 2.2 of Ryan et al. (2018):

"A common way of conducting global sensitivity analysis for each point in the output space of the simulator – where the output consists of, for example, a spatial map or a time series – is to compute the first-order sensitivity indices (SIs) using variance-based decomposition; this apportions the variance in simulator output (a scalar) to different sources of variation in the different model inputs. Assuming the input variables are independent of one another – which they are for this study – the first-order SI, corresponding to the i^{th} input variable ($i = 1, 2, ..., p$) and the j^{th} point in the output space, is given by the equation (R1).

$$SI_{i,j} = \frac{\mathrm{Var}[\mathrm{E}(Y_j \mid X_i)]}{\mathrm{Var}(Y_j)} \times 100 \qquad (R1)$$

where X_i is the i^{th} column of the $n \times p$ matrix X (i.e. a matrix with n rows and p columns) which stores the n samples of p-dimensional inputs, and Y_j is the j^{th} column of the $n \times m$ matrix which stores the corresponding n sets of m-dimensional outputs. We multiply by 100 so that the SI is given as a percentage. The notation given by Var(•) and E(•) denotes the mathematical operations that compute the variance and expectation. The simplest way of computing $SI_{i,j}$ is by brute force, but this is also the most computationally intensive."

Source from: the section 2.2 of Ryan et al., (2018)

Description of eFAST method in the section 2.2.2 of Ryan et al. (2018):

"The eFAST method is an alternative and more efficient way of estimating the terms in Eq. (R1). A multi-dimensional Fourier transformation of the simulator f, allows a variance-based decomposition that samples the input space along a curve defined by the equation (R2).

$$x_i(s) = G_i(\sin(\omega_i s)) \qquad (R2)$$

where x =(x1, ..., xp) refers to a general point in the input space that has been sampled, $s \in R$ is a variable over the range $(-\infty, \infty)$, G_i is the i^{th} transformation function, and ω_i is the i^{th} user-specified frequency corresponding to each input. Varying s allows a multi-dimensional exploration of the input space due to the $x_i(s)$ being simultaneously varied. Depending on the simulator, we typically require n=1000–10,000 samples from the input space. After applying the simulator f, the resulting scalar output – denoted generally by y – produces different periodic functions based on different ω_i. If the output y is sensitive to changes in the i^{th} input factor, the periodic function of y corresponding to frequency ω_i will have a high amplitude."

Source from: the section 2.2.2 of Ryan et al., (2018)

Please refer to the section 2.2.2 of Ryan et al. (2018) for more specific details about the theory and equations of eFAST method. In order not to replicate many mathematic equations in Ryan et al. (2018), in this study, we have rephrased the section 2.3 to summarize the advantage of global sensitivity analysis compared with the widely used 'one-at-a-time' sensitivity analysis and to simply describe how we perform GSA with non-mathematic language. The detailed modifications of section 2.3 are shown in the point-4, combining with the responses to the points 2-4.

4) Line 188: Similarly, "Gaussian process emulation" is not sufficiently well described in the manuscript. A summary of how this technique works and how it is applied must be included.

To perform global sensitivity analysis and generate response surfaces, which describe relationships between the inputs and outputs of models, usually requires thousands of model runs. This is not feasible for a computationally expensive model like WRF-Chem. Therefore, in our study a Gaussian process (GP) emulator, trained by a few model runs, is used as a surrogate of WRF-Chem model. Mathematically, an emulator is a statistical model that mimics

the input-output relationship of a simulator, i.e., the expensive WRF-Chem model in this study. The most common form of an emulator is a GP emulator since it has attractive mathematical properties that allow an analytical derivation of the mean and variance of the emulated output (Ryan et al., 2018). As summarized in Ryan et al. (2018):

> *"More formally, a GP is an extension of the multivariate Gaussian distribution to infinitely many variables (Rasmussen and Williams, 2006). The multivariate Gaussian distribution is specified by a mean vector and covariance matrix. A GP has a mean function which is typically given by* $m(x) = \mathrm{E}(\mathrm{f}(\mathrm{x}))$ *and covariance function given by* $c(x, x') = cov(f(x), f(x'))$*".*
>
> ***Source from: Ryan et al., (2018)***
>
> *Where x and x' are two different input-matrix.*

Detailed theory of GP emulation is introduced in an open-accessible methodological study (Ryan et al., 2018), and equations and the R code for generating GP emulator are also given in Ryan et al. (2018). In our manuscript, we have substantially revised the section 2.3 to summarize the GP emulator with non-mathematical language, and to describe its advantages and how we use it. The revised section 2.3 is shown below, please also find detailed changes in the revise-tracked file.

Revised section 2.3 of this study:

"2.3 Global Sensitivity Analysis of Urban Air Pollution

We perform global sensitivity analysis (GSA) (Iooss and Lemaître, 2015) to quantify the sensitivity of modelled outputs ($PM_{2.5}$ and O_3 for this study) to changes in the model inputs, which for this study are emissions from the different emission sectors. One-at-a-time sensitivity analysis is a common way of calculating model sensitivity and involves varying a single model

input while the other inputs are fixed at nominal values, e.g., Wild (2007). While one-at-a-time approach is relatively easy to implement, it assumes that the model response to different inputs is independent and this can lead to biased results (Saltelli et al., 1999;Pisoni et al., 2018;Carslaw et al., 2013). GSA overcomes the problems of the one-at-a-time approach by averaging over the other inputs rather than fixing them at specific values. This allows calculation of first-order sensitivity indices (SIs) for each variable, corresponding to the i^{th} input variable and the j^{th} output point, is given by the Eq. 1 (Ryan et al., 2018).

$$SI_{i,j} = \frac{Var[E(y_j \mid x_i)]}{Var(y_j)} \times 100\% \qquad (1)$$

where x_i is the i^{th} element of the input; and y_j is the j^{th} element of the output. The 'E(•)' and 'Var(•)' denote the mathematical function that calculate the expectation and variance, respectively. The simplest way of computing $SI_{i,j}$ is by brute force, but this is also the most computationally intensive (Ryan et al., 2018).

The extended Fourier Amplitude Sensitivity Test (eFAST), first developed by Saltelli et al. (1999), is a commonly used approach to perform GSA and calculate SIs and is adopted in this study because of its high efficiency. A basic overview and detailed equations of the eFAST method are given in the section 2.2.2 of Ryan et al. (2018). A challenge to using eFAST is that it typically requires thousands of model runs. To overcome this, we employ a computationally cheaper surrogate model in place of our expensive simulation model WRF-Chem. A surrogate model is a simple model (usually statistical) which can map the inputs to the outputs of the simulation model with sufficiently good accuracy given the same inputs. In this study, we choose a type of surrogate model called a Gaussian process emulator, which works like a function for multi-dimensional interpolation and has been used extensively in many areas of applied science (Carslaw et al., 2013;Koehler and Owen, 1996;Queipo et al., 2005;Vanuytrecht

and Willems, 2014;vu et al., 2015;Degroote et al., 2012) and uncertainty assessment of atmospheric models (Lee et al., 2016;Lee et al., 2012;Lee et al., 2011). Gaussian process emulators typically require a relatively small number of runs of the computational-expensive model to generate; this is in contrast to other surrogate modelling approaches, such as neural networks, which typically require thousands of model runs to train them. For a basic overview of a Gaussian process emulator see O'Hagan (2006), detailed introduction and equations are also given in the section 2.3 of Ryan et al. (2018). Before using the emulator in place of the WRF-Chem model to carry out the thousands of model runs required for GSA, we train the emulator using a relatively small number of WRF-Chem model runs. Following previous studies (Carslaw et al., 2013;Lee et al., 2016), a Maximin Latin hypercube space-filling design is employed to select the designs of training runs for WRF-Chem. Latin hypercube sampling is a statistical method for generating a near-random sample of parameter values from a multidimensional distribution (Shields and Zhang, 2016). Here, we search through 100,000 Latin hypercube random designs to find the optimal one where the parameter space is filled most effectively. This ensures that the sets of inputs chosen cover as large a fraction of the input space as possible. Full details (including R codes) of how to generate the Gaussian process emulator, eFAST method and GSA can be found in Ryan et al. (2018).*"*

5) Lines 209-210: "10,000 random samples" are performed to check that the emulator "can fully represent the results of WRF-Chem". Does this mean that the authors performed 10,000 runs of WRF-Chem, and compared them with 10,000 runs of the emulator? Or did they do something else? What do each of the points in Fig. 3 actually represent? This is not clear at all. The authors seem to be relying on this analysis to show that the emulation "provides a good representation of the model", but in my opinion this has not been shown at all. Much more detail is needed here.

The "10,000 random samples" refers to selection of 10,000 samples from the spatial grid cells and temporal duration of the model run and rebuilding emulators at these points using all but

one of the WRF-Chem model training runs, and then comparing these against results from the model run that was omitted in 'leave-one-out' cross-validation. This provides an independent check of how well Gaussian process emulator can represent the results of WRF-Chem. And, thanks to reviewer's suggestion in the last comment, the further validation with the base and regional joint reduction cases also demonstrate good agreement between the emulator and WRF-Chem model (see response to the last comment). We have modified the corresponding context in the last part of section 2.3 to make this clearer, as shown below.

"We perform 'leave-one-out' cross-validation (O'Hagan and West, 2009;Wang et al., 2011) with 10,000 random samples to check that the Gaussian process emulator can fully represent the results of WRF-Chem."

Changed to:

" The accuracy of the emulator as a surrogate of WRF-Chem model is evaluated using a 'leave-one-out' cross-validation (Bastos and O'Hagan, 2009). This involves training the emulator using 19 out of the 20 sets of inputs/outputs from the WRF-Chem model runs and then evaluating the emulator against the 20^{th} simulation. This process is carried out for each of the 20 sets of inputs/outputs. Given that the output space is multi-dimensional (i.e. modelled O_3 and $PM_{2.5}$ varied spatially and in time), the validation of the emulator by comparing 10,000 (random-samples varied spatially and in time) of emulator output values against the corresponding output values of the WRF-Chem model. The emulator validation plot is shown in Fig. 3. Modelled and emulated O_3 and $PM_{2.5}$ lie very close to the 1:1 line with R^2 values of more than 95% as shown in Fig. 3, indicating that the emulation provides an accurate representation of the input-output relationship of the WRF-Chem model."

6) Line 256: NOx appears to be significantly underestimated by WRF-Chem during the middle of the day, when peak ozone concentrations are also modelled. Given the central role of NOx as an ozone precursor, it appears that the modelled peak ozone is being well simulated for the wrong reasons. There is likely a compensating error in some other aspect of the model. The

authors should provide some discussion about how these errors in WRF-Chem would propagate into their emulator and affect the global sensitivity analysis.

Thank you for pointing this out. The choice of y-axis range in Fig. S4 was not fully appropriate and makes NOx looks significantly underestimated by WRF-Chem during the middle of the day when peak ozone occurs. We have changed the y-axis range to [0 200], more in line with convention, as shown below. Instead of a "remarkable underestimation", the NOx is actually underestimated by only ~30%. The daytime variation of NOx (Fig. S4) is directly opposite in pattern to that of boundary layer height (red dashed line in Fig. 4a) between 9 am and 6 pm, suggesting that this underestimation in NOx is closely associated with the variation in boundary layer behavior, a substantial uncertainty in the simulation for which no observational verification is available.

The reviewer is right that the good simulation of peak O_3 when NOx is underestimated highlights an uncertainty within the model. This uncertainty would propagate into the emulator and affect the global sensitivity analysis, because emulator learns from the WRF-Chem model and reproduces whatever the model outputs. We have added discussion about this influence in the sections 3.4 and 3.5, as shown below.

In the section 3.4 of revised version:

"NOx, mainly originating from traffic emissions, is underestimated by ~30% during the O_3 peak period (Fig. S4). This uncertainty can propagate into the Gaussian process emulator and could lead to underestimation of the influence of traffic on peak O_3, but is not expected to change the nature of our conclusions about the predominance of regional transport and local traffic emissions."

In the section 3.5 of revised version:

"We note that our model may underestimate the influence of traffic emissions on O_3 to some extent as described above (section 3.4), suggesting that the ozone increase could be stronger than we predict. To prevent the side-effect of increasing O_3 by controls on traffic emissions…"

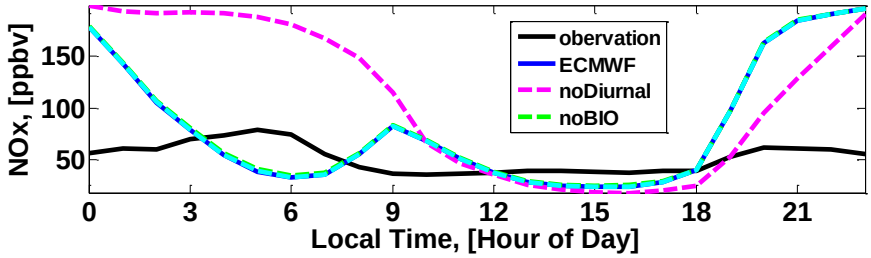

Original Figure S4. *Diurnal patterns of NOx concentration from WRF-Chem model and observational results at AIR site. The results are averaged during 02-15 May 2015. Note that 'ECMWF' indicates the model results driven by ECMWF reanalysis data.*

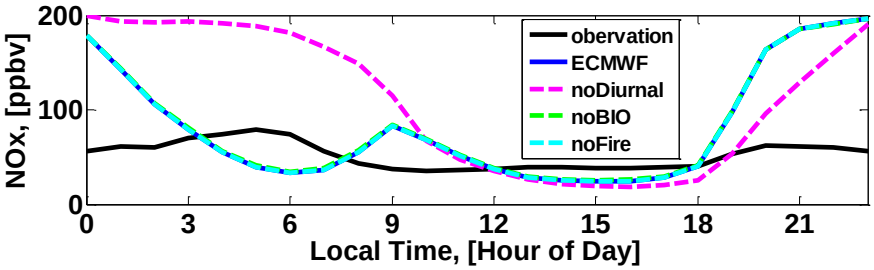

Revised Figure S4. *Diurnal patterns of NOx concentration from WRF-Chem model and observational results at AIR site. The results are averaged during 02-15 May 2015. Note that 'ECMWF' indicates the model results driven by ECMWF reanalysis data.*

7) Line 267: "We remove these sources". From what? WRF-Chem itself, or the emulator?

We have revised the statement, as shown below.

"We turn off these sources in the WRF-Chem simulation".

8) Lines 311-312 and Fig. 5b: It should be pointed out somewhere in the discussion that the overwhelming dominance of traffic NOx emissions on ozone in Delhi is actually through anti-correlation. Presenting the sensitivity indices of "TRA" and "NCR" together on the same plot is potentially quite misleading unless the authors make it clear that their respective influences have opposite sign.

The reviewer is right that "overwhelming dominance of traffic NOx emissions on ozone in Delhi is actually through anti-correlation.". Although we have already explained this anti-correlation relationship in section 3.4:

"Traffic contributes ~75% of total NOx emission in Delhi (Fig. 6b), and the shallow PBL during the night traps the NOx. This removes O_3 through chemical reaction".

This may not be clear enough. We have added description at the beginning of this section to make this point clearer, as shown below. Thanks for pointing this out.

"The variation of O_3 in Delhi City Region is overwhelmingly dominated by local traffic emissions with a sensitivity index higher than 80% at night-time (Fig. 5b), where O_3 and traffic emissions are anti-correlated."

9) Section 3.5: This is a nice example of the potential power and utility of the methodology. Figure 7d is an especially clear illustration of the emissions control trajectory which is required to prevent an increase in ozone in Delhi despite reducing local NOx emissions. As mentioned in my general comments, this general approach to emission control (reducing ozone by focusing on regional-scale emissions) is consistent with current understanding of ozone chemistry, so this result by itself is rather unremarkable. What is really interesting here is the ability to rapidly discover an optimal emission mitigation pathway, and quantify its effects. What is missing here though, is a verification that the same combined emission controls for TRA and NCR would result in the same reductions in PM and ozone when employed in the full WRF-Chem model. It would only take one WRF-Chem run to verify this result. In my opinion this extra run is necessary for the authors to be able to show that their approach really is capable of what they claim.

This is a good point. This one extra WRF-Chem simulation makes the verification of emulator more solid and evident. We have performed the extra simulation as suggested. In addition, we also compare the base case (without change of emissions) WRF-Chem results against the emulator results. Noting that the base case is not part of the training cases for emulator, see a list of training cases in Table S2; therefore, this comparison also provides an independent validation for the GP emulator. The results of WRF-Chem and emulator show almost the same reductions in the joint control case. As shown in the figure below, the emulator does reproduce

the WRF-Chem simulation nicely, with an uncertainty (normalized mean error) of less than 5% and R^2 higher than 0.95 for both $PM_{2.5}$ and O_3. Thanks for the suggestion, we have added this extra validation in the section 3.5, as shown below.

"We test this by performing an additional run with WRF-Chem using emission reductions of 50% and 30% for sectors of local traffic and the surrounding NCR region, respectively. We compare the WRF-Chem results of the additional run and the base case (without change of emissions) against the corresponding results from Gaussian process emulator (Fig. S8). We find that the $PM_{2.5}$ and O_3 results from the model runs lie within 5% of those estimated with the emulator and with R^2 higher than 95%, demonstrating the high quality of the emulation approach adopted here and underlining its deeper value for identifying mitigation approaches"

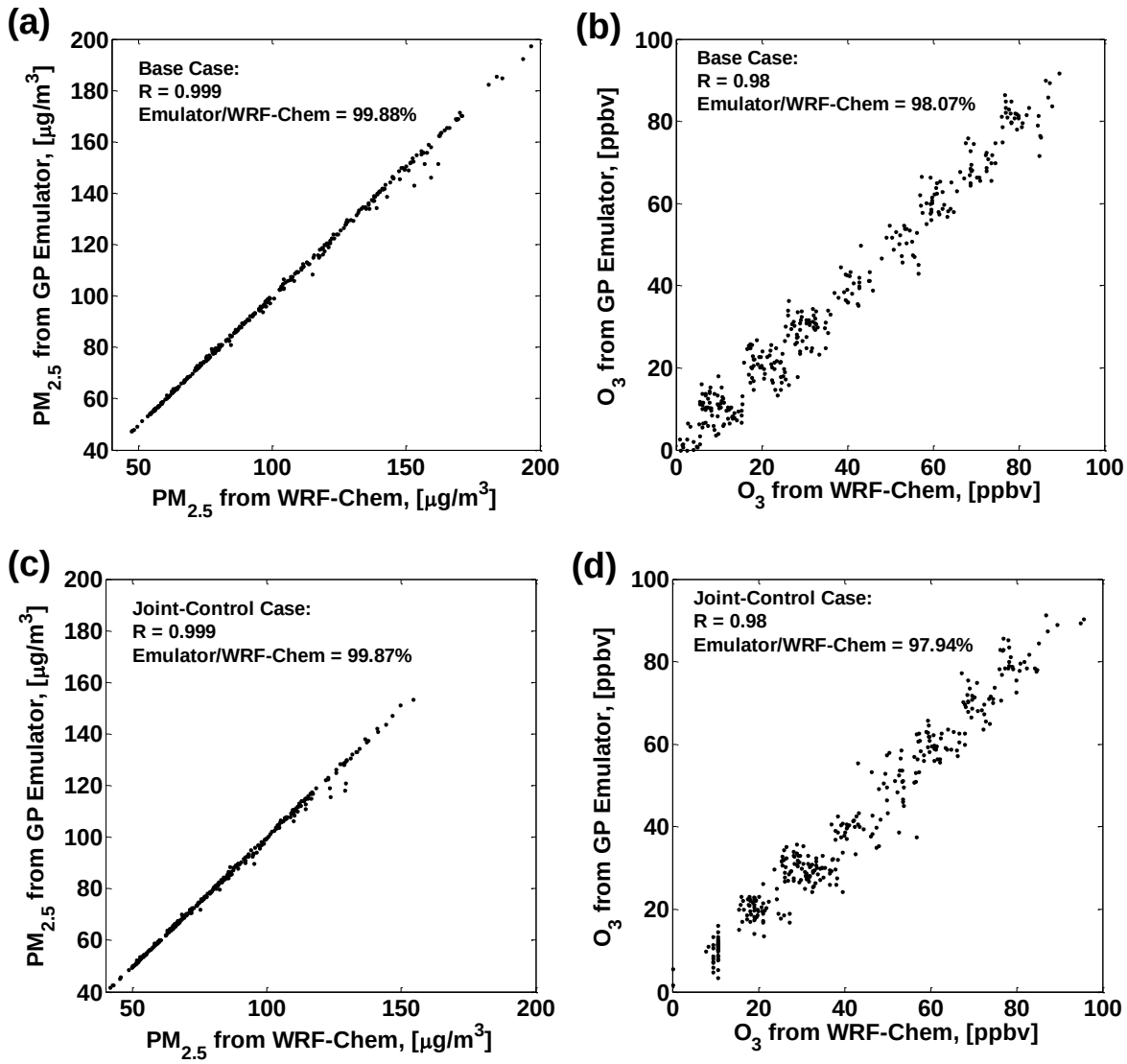

Newly added Figure S8. *Extra validation of Gaussian process emulator results in the mitigation strategy according to Fig. 7. The accuracy of the emulator for reproducing*

*current conditions of $PM_{2.5}$ **(a)** and O_3 **(b)**, i.e. base case without changing emissions. The accuracy of the emulator for reproducing regional joint coordination conditions of $PM_{2.5}$ **(c)** and O_3 **(d)**, i.e. NCR joint control case with local traffic emissions reduced by 50% and regional emissions reduced by 30%. All the results are averaged over Delhi City Region, with hourly resolution during the simulation period.*

References:

Carslaw, K. S., Lee, L. A., Reddington, C. L., Pringle, K. J., Rap, A., Forster, P. M., Mann, G. W., Spracklen, D. V., Woodhouse, M. T., Regayre, L. A., and Pierce, J. R.: Large contribution of natural aerosols to uncertainty in indirect forcing, Nature, 503, 67, 10.1038/nature12674, 2013.

Dee, D. P., Uppala, S. M., Simmons, A. J., Berrisford, P., Poli, P., Kobayashi, S., Andrae, U., Balmaseda, M. A., Balsamo, G., Bauer, P., Bechtold, P., Beljaars, A. C. M., van de Berg, L., Bidlot, J., Bormann, N., Delsol, C., Dragani, R., Fuentes, M., Geer, A. J., Haimberger, L., Healy, S. B., Hersbach, H., Hólm, E. V., Isaksen, L., Kållberg, P., Köhler, M., Matricardi, M., McNally, A. P., Monge-Sanz, B. M., Morcrette, J.-J., Park, B.-K., Peubey, C., de Rosnay, P., Tavolato, C., Thépaut, J.-N., and Vitart, F.: The ERA-Interim reanalysis: configuration and performance of the data assimilation system, Quarterly Journal of the Royal Meteorological Society, 137, 553-597, 10.1002/qj.828, 2011.

Degroote, J., Couckuyt, I., Vierendeels, J., Segers, P., and Dhaene, T.: Inverse modelling of an aneurysm's stiffness using surrogate-based optimization and fluid-structure interaction simulations, Structural and Multidisciplinary Optimization, 46, 457-469, 10.1007/s00158-011-0751-7, 2012.

Iooss, B., and Lemaître, P.: A review on global sensitivity analysis methods. In: Meloni, C., Dellino, G. (Eds.), Uncertainty Management in Simulationoptimization of Complex Systems: Algorithms and Applications. Springer, 2015.

Koehler, J. R., and Owen, A. B.: 9 Computer experiments, in: Handbook of Statistics, Elsevier, 261-308, 1996.

Lee, L. A., Carslaw, K. S., Pringle, K. J., Mann, G. W., and Spracklen, D. V.: Emulation of a complex global aerosol model to quantify sensitivity to uncertain parameters, Atmos. Chem. Phys., 11, 12253-12273, 10.5194/acp-11-12253-2011, 2011.

Lee, L. A., Carslaw, K. S., Pringle, K. J., and Mann, G. W.: Mapping the uncertainty in global CCN using emulation, Atmos. Chem. Phys., 12, 9739-9751, 10.5194/acp-12-9739-2012, 2012.

Lee, L. A., Reddington, C. L., and Carslaw, K. S.: On the relationship between aerosol model uncertainty and radiative forcing uncertainty, Proceedings of the National Academy of Sciences, 113, 5820-5827, 10.1073/pnas.1507050113, 2016.

O'Hagan, A.: Bayesian analysis of computer code outputs: A tutorial, Reliability Engineering & System Safety, 91, 1290-1300, https://doi.org/10.1016/j.ress.2005.11.025, 2006.

O'Hagan, A., and West, M.: Handbook of applied Bayesian analysis, Oxford University Press, New York, 2009.

Pisoni, E., Albrecht, D., Mara, T. A., Rosati, R., Tarantola, S., and Thunis, P.: Application of uncertainty and sensitivity analysis to the air quality SHERPA modelling tool, Atmospheric Environment, 183, 84-93, https://doi.org/10.1016/j.atmosenv.2018.04.006, 2018.

Queipo, N. V., Haftka, R. T., Shyy, W., Goel, T., Vaidyanathan, R., and Kevin Tucker, P.: Surrogate-based analysis and optimization, Progress in Aerospace Sciences, 41, 1-28, https://doi.org/10.1016/j.paerosci.2005.02.001, 2005.

Rasmussen, C. E., and Williams, C. K. I.: Gaussian Processes for Machine Learning, the MIT Press, ISBN 026218253X, 2006.

Ryan, E., Wild, O., Voulgarakis, A., and Lee, L.: Fast sensitivity analysis methods for computationally expensive models with multi-dimensional output, Geosci. Model Dev., 11, 3131-3146, 10.5194/gmd-11-3131-2018, 2018.

Saltelli, A., Tarantola, S., and Chan, K. P. S.: A Quantitative Model-Independent Method for Global Sensitivity Analysis of Model Output, Technometrics, 41, 39-56, 10.1080/00401706.1999.10485594, 1999.

Shields, M. D., and Zhang, J.: The generalization of Latin hypercube sampling, Reliability Engineering & System Safety, 148, 96-108, https://doi.org/10.1016/j.ress.2015.12.002, 2016.

Vanuytrecht, E., and Willems, P.: Global sensitivity analysis of yield output from the water productivity model, Environmental Modelling and Software, 51, 323-332, 10.1016/j.envsoft.2013.10.017, 2014.

vu, N., Rafiee, R., Zhuang, X., Lahmer, T., and Rabczuk, T.: Uncertainty quantification for multiscale modeling of polymer nanocomposites with correlated parameters, Composites Part B: Engineering, 68, 446-464, 10.1016/j.compositesb.2014.09.008, 2015.

Wang, S., Xing, J., Jang, C., Zhu, Y., Fu, J. S., and Hao, J.: Impact Assessment of Ammonia Emissions on Inorganic Aerosols in East China Using Response Surface Modeling Technique, Environmental Science & Technology, 45, 9293-9300, 10.1021/es2022347, 2011.

Wild, O.: Modelling the global tropospheric ozone budget: exploring the variability in current models, Atmos. Chem. Phys., 7, 2643-2660, 10.5194/acp-7-2643-2007, 2007.

Response to comments of referee #2

General comments

This manuscript uses Gaussian process emulation to generate a efficient surrogate for WRF-Chem to perform the sensitivity analysis of PM2.5 and O3 to sources, and to provide air pollution mitigation suggestions. The combination of WRF-Chem with Gaussian process emulation is novel to reduce computational complexity for sensitivity analysis. The results, especially the joint control suggestions for PM2.5 and O3, are useful in terms of air pollution control. The manuscript is well written, but some parts of it are not clear enough. I would recommend for publication after the authors address the following specific comments:

Many thanks to the reviewer for the comments and suggestions. We have improved the manuscript accordingly. Please find a point-by-point response below.

Specific comments:

1) Line 45: please add references for this statement: Menon, S., Hansen, J., Nazarenko, L. and Luo, Y., 2002. Climate effects of black carbon aerosols in China and India. Science, 297(5590), pp.2250-2253. Gao, M., Sherman, P., Song, S., Yu, Y., Wu, Z. and McElroy, M.B., 2019. Seasonal prediction of Indian wintertime aerosol pollution using the ocean memory effect. Science advances, 5(7), p.eaav4157.

Thanks for the useful references. We have added these references (Menon et al., 2002;Gao et al., 2019) as suggested.

2) Line 81: Is it possible to provide a clear definition of pollutant response surface?

We have added a description of pollutant response surface in the introduction, as shown below.

"The response surfaces describe that how the pollutants, i.e., $PM_{2.5}$ and O_3, will respond to the changes in emissions from different sectors."

3) Line 130-132: This statement is a bit general. Better to use measurements of precipitation and clouds to show this point.

There is no precipitation in Delhi during the simulation period. We have added this statement in the revised version. The climatic averaged monthly precipitation during May in Delhi is only about 20 mm (https://weather-and-climate.com/average-monthly-precipitation-Rainfall,New-Delhi,India).

4) Fig. 6: Better to provide similar plots for other important species, such as organics, SO2, etc.

We have added similar plots for black carbon, non-methane VOC, organic carbon and SO_2 in Figure S13, as shown below.

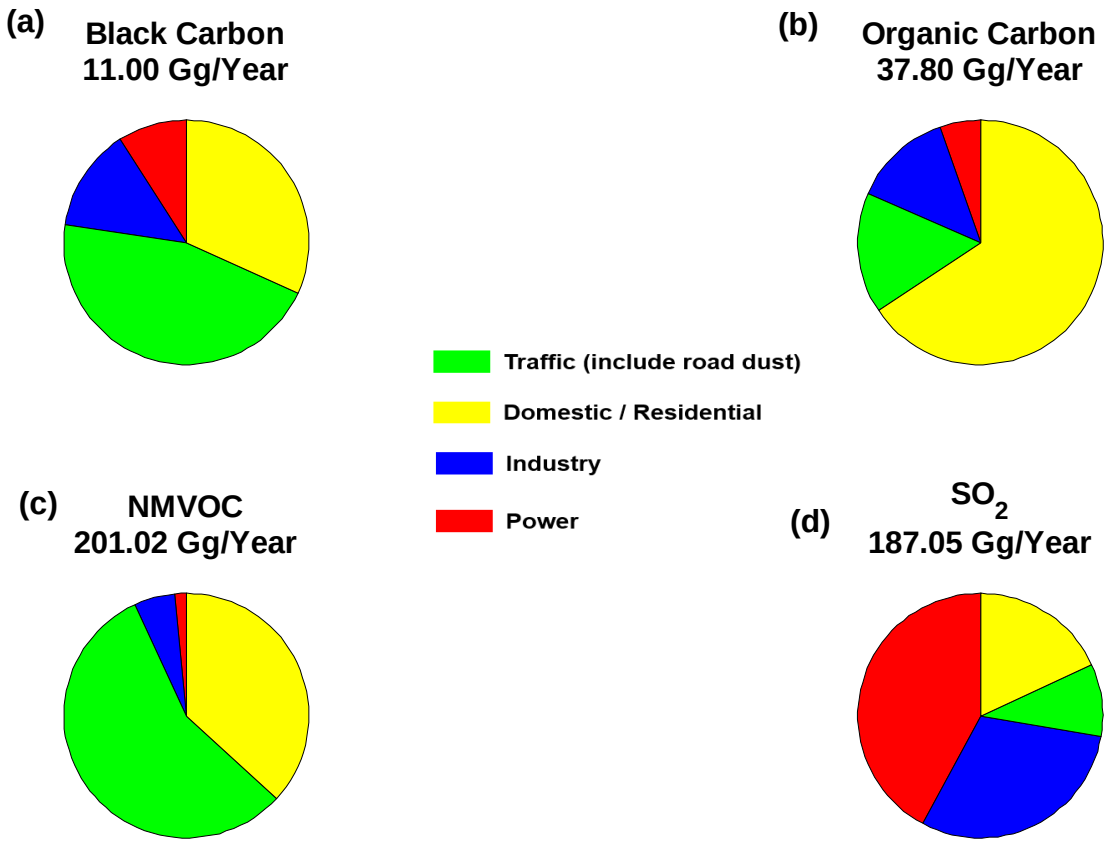

Figure S13. *Annual emission of different sectors in Delhi from SAFAR inventory. (a) black carbon; (b) organic carbon; (c) non-methane VOC and (d) SO_2.*

5) Sect 4: It would be better to compare the results with other similar studies and explain the similarities and differences.

Thanks for the suggestion. We have revised the corresponding context in Section 4 to include a comparison with other similar studies. The revised version is shown below, please also see the change-tracked file for more details.

"They co-dominate the O_3 peak and $PM_{2.5}$ in Delhi during daytime, while the regional transport governs $PM_{2.5}$ during the night, in line with a recent study showing that ~60% of $PM_{2.5}$ in Delhi originates from outside (Amann et al., 2017). Controlling local traffic emissions in Delhi would have the notable side effect of increasing O_3, at least in the pre-monsoon/summer period (peak O_3 season) that we consider here. This is in line with recent increases in O_3 seen in China (Silver et al., 2018;Li et al., 2018). The Chinese experience suggests that regional joint coordination is required to effectively mitigate PM2.5 pollution in Beijing (Liu et al., 2016). Our pollutant response surfaces go one step further and suggest that joint coordinated emission controls with the NCR region surrounding Delhi would be required to not only achieve a more ambitious reduction of $PM_{2.5}$ but also to minimize the risk of O_3 increases."

References:

Amann, M., Purohit, P., Bhanarkar, A. D., Bertok, I., Borken-Kleefeld, J., Cofala, J., Heyes, C., Kiesewetter, G., Klimont, Z., Liu, J., Majumdar, D., Nguyen, B., Rafaj, P., Rao, P. S., Sander, R., Schöpp, W., Srivastava, A., and Vardhan, B. H.: Managing future air quality in megacities: A case study for Delhi, Atmospheric Environment, 161, 99-111, https://doi.org/10.1016/j.atmosenv.2017.04.041, 2017.

Gao, M., Sherman, P., Song, S., Yu, Y., Wu, Z., and McElroy, M. B.: Seasonal prediction of Indian wintertime aerosol pollution using the ocean memory effect, Science Advances, 5, eaav4157, 10.1126/sciadv.aav4157, 2019.

Li, K., Jacob, D. J., Liao, H., Shen, L., Zhang, Q., and Bates, K. H.: Anthropogenic drivers of 2013–2017 trends in summer surface ozone in China, Proceedings of the National Academy of Sciences, 201812168, 10.1073/pnas.1812168116, 2018.

Liu, J., Mauzerall, D. L., Chen, Q., Zhang, Q., Song, Y., Peng, W., Klimont, Z., Qiu, X., Zhang, S., Hu, M., Lin, W., Smith, K. R., and Zhu, T.: Air pollutant emissions from Chinese households: A major and underappreciated ambient pollution source, Proceedings of the National Academy of Sciences, 113, 7756-7761, 10.1073/pnas.1604537113, 2016.

Menon, S., Hansen, J., Nazarenko, L., and Luo, Y.: Climate Effects of Black Carbon Aerosols in China and India, Science, 297, 2250-2253, 10.1126/science.1075159, 2002.

Silver, B., Reddington, C. L., Arnold, S. R., and Spracklen, D. V.: Substantial changes in air pollution across China during 2015–2017, Environmental Research Letters, 13, 114012, 10.1088/1748-9326/aae718, 2018.

Mitigation of $PM_{2.5}$ and Ozone Pollution in Delhi: A Sensitivity Study during the Pre-monsoon period

Ying Chen[1,2*], Oliver Wild[1,2], Edmund Ryan[1,9], Saroj Kumar Sahu[4], Douglas Lowe[5], Scott Archer-Nicholls[6], Yu Wang[5], Gordon McFiggans[5], Tabish Ansari[1], Vikas Singh[7], Ranjeet S. Sokhi[8], Alex Archibald[6], Gufran Beig[3]

[1]Lancaster Environment Centre, Lancaster University, Lancaster, LA1 4YQ, UK

[2]Data Science Institute, Lancaster University, Lancaster, LA1 4YW, UK

[3]Indian Institute of Tropical Meteorology, Pune, India

[4]Environmental Science, Dept. of Botany, Utkal University, Bhubaneswar, India

[5]Centre for Atmospheric Sciences, School of Earth, Atmospheric and Environmental Sciences, University of Manchester, Manchester, UK

[6]NCAS-Climate, Department of Chemistry, University of Cambridge, Cambridge, UK

[7]National Atmospheric Research Laboratory, Gadanki, AP, India

[8]Centre for Atmospheric and Climate Physics Research, University of Hertfordshire, Hatfield, Hertfordshire, UK

[9]School of Mathematics, University of Manchester, Manchester, UK

Correspondence to: Ying Chen (y.chen65@lancaster.ac.uk)

Abstract:

Fine particulate matter ($PM_{2.5}$) and surface ozone (O_3) are major air pollutants in megacities such as Delhi, but the design of suitable mitigation strategies is challenging. Some strategies for reducing $PM_{2.5}$ may have the notable side-effect of increasing O_3. Here, we demonstrate a numerical framework for investigating the impacts of mitigation strategies on both $PM_{2.5}$ and O_3 in Delhi. We use Gaussian process emulation to generate a computationally efficient surrogate for a regional air quality model (WRF-Chem). This allows us to perform global sensitivity analysis to identify the major sources of air pollution, and to generate emission-sector based pollutant response surfaces to inform mitigation policy development. Based on more than 100,000 emulation runs during the pre-monsoon period (peak O_3 season), our global sensitivity analysis shows that local traffic emissions from Delhi city region and regional transport of pollutions emitted from the National Capital Region surrounding Delhi (NCR) are dominant factors influencing $PM_{2.5}$ and O_3 in Delhi. They together govern the O_3 peak and $PM_{2.5}$ concentration during daytime. Regional transport contributes about 80% of the $PM_{2.5}$ variation during the night. Reducing traffic emissions in Delhi alone (e.g., by 50%) would reduce $PM_{2.5}$ by 15-20% but lead to a 20-25% increase in O_3. However, we show that reducing NCR regional emissions by 25-30% at the same time would further reduce $PM_{2.5}$ by 5-10% in Delhi and avoid the O_3 increase. This study provides scientific evidence to support the need for joint coordination of controls on local and regional scales to achieve effective reduction ~~o~~in $PM_{2.5}$ whilst minimizing~~e~~ the risk of O_3 increase in Delhi.

1. Introduction

Exposure to air pollutants increases morbidity and mortality (Huang et al., 2018a;WHO, 2013). The urban air quality in India, especially in Delhi, is currently among the poorest in the world (WHO, 2013, 2016a, b). In addition to the local impacts, the Indian monsoon can transport air pollutants to remote oceanic regions, inject them into the stratosphere and redistribute them globally (Lelieveld et al., 2018). This makes the impact of Indian air pollution wide ranging regionally and globally ~~as well as having~~and it has interactions with climate and ecosystems world-wide (Menon et al., 2002;Gao et al., 2019).

$PM_{2.5}$ (particulate matter with an aerodynamic diameter of less than 2.5 μm) is a major air pollutant, causing increases in disease (Pope et al., 2009;Gao et al., 2015;Stafoggia et al., 2019) and reduced visibility (Mukherjee and Toohey, 2016;Wang and Chen, 2019;Khare et al., 2018). The population of India experiences high $PM_{2.5}$ exposure, and this is responsible for ~1 million premature deaths per year (Conibear et al., 2018;Gao et al., 2018). Residential emissions are estimated to contribute ~50% of $PM_{2.5}$ concentrations and to cause more than 0.5 million annual mortalities across India (Conibear et al., 2018). ~~The World Health Organization (WHO) reported~~Previous studies reported an annual averaged $PM_{2.5}$ loading of ~~~~110-140 μg/m^3 in Delhi during~~in~~ 2015-2018~~6~~, leading to ~10,000 premature deaths per year in the city (Chen et al., 2019; Chowdhury and Dey, 2016; WHO, 2016a). In Delhi, the traffic sector (~50%) and the domestic sector (~20%) are the major local contributors to $PM_{2.5}$ (Marrapu et al., 2014). Efforts to control traffic emissions in Delhi in recent years by introducing an alternating 'odd-even' licence plate policy have led to reductions in $PM_{2.5}$ of less than 10% (Chowdhury et al., 2017). This indicates that there is an urgent need for a coordinated plan to mitigate $PM_{2.5}$ pollution (Chowdhury et al., 2017).

Surface ozone (O_3), another major air pollutant, is damaging to health and reduces crop yields (Ashworth et al., 2013;Lu et al., 2018;Kumar et al., 2018). The risks of respiratory and cardiovascular diseases are increased from short-term exposure to high ambient O_3 and from long-term exposure at low levels (WHO, 2013;Turner et al., 2016;Fleming et al., 2018). Oxidation of volatile organic compounds (VOCs) in the presence of nitrogen oxides (NOx) is the main source of surface ozone. Rapid economic development in India has greatly increased the emissions of these O_3 precursors (Duncan et al., 2016), leading to significant increases in O_3 especially during the pre-monsoon period (Ghude et al., 2008). Hourly maximum O_3 reaches as much as 140 ppbv during the pre-monsoon season in Delhi (Ghude et al., 2008), comparable to the most polluted regions in China (150 ppbv, Wang et al., 2017) and higher than the most polluted areas in the U.S. (110 ppbv, Lu et al., 2018).

Mitigation of $PM_{2.5}$ pollution may lead to an increase in surface ozone, because the dimming effect of aerosols and removal of hydroperoxy radicals are reduced, facilitating O_3 production (Huang et al., 2018b;Li et al., 2018;Hollaway et al., 2019). Furthermore, co-reduction of NOx and $PM_{2.5}$ emissions may increase O_3 in cities where O_3 production is in a VOC-limited photochemical regime (Ran et al., 2009;Xing et al., 2018;Xing et al., 2017). This has recently been reported in a number of Asian megacities, e.g. Shanghai (Silver et al., 2018), Beijing (Wu et al., 2015;Liu et al., 2017;Chen et al., 2018) and Guangzhou (Liu et al., 2013). Delhi and coastal cities in India, which are known to be VOC-limited (Sharma et al., 2017), may face increased O_3 as a side-effect of emission controls focused on $PM_{2.5}$. Therefore, studies of mitigation strategies that target both $PM_{2.5}$ and O_3 are urgently needed (Chen et al., 2018), particularly as urban air pollution in India has been much less well studied than in many other countries.

To investigate the impacts of mitigation strategies with respect to both $PM_{2.5}$ and O_3, we demonstrate a framework for generating emission-sector based pollutant response surfaces using Gaussian process emulation (O'Hagan and West, 2009;O'Hagan, 2006). The response surfaces describe that how the pollutants, i.e., $PM_{2.5}$ and O_3, will respond to the changes in emissions from different sectors. We conduct global sensitivity analysis to identify the dominant emission sectors controlling $PM_{2.5}$ and O_3, and then generate sector based response surfaces to quantify the impacts on $PM_{2.5}$ and O_3 of emission reductions. In contrast to simple sensitivity analysis varying one input at a time, this allows full exploration of the entire input space, accounting for the interactions between different inputs (Pisoni et al., 2018;Saltelli et al., 1999). Conventionally, chemical transport models (CTMs~~, e.g. WRF-Chem~~) are used to calculate the impacts on pollutants concentrations of different mitigation scenarios. However, the computational expensive of CTMs makes them unsuitable for performing global sensitivity analysis or generating response surfaces, which usually require thousands of model runs. To overcome this difficulty, source-receptor relationships (Amann et al., 2011) or computational efficient surrogate models, trained on a limited number of CTM simulations, are used to replace the expensive CTM. These approaches have been used to perform sensitivity and uncertainty analysis of regional air quality models (Pisoni et al., 2018), assessment of regional air quality plans (Zhao et al., 2017;Xing et al., 2017;Pisoni et al., 2017;Thunis et al., 2016) and sensitivity and uncertainty analysis of global and climate simulations (Ryan et al., 2018;Lee et al., 2016;Lee et al., 2012). Here, we use surrogate model to explore the sensitivity of $PM_{2.5}$ and O_3 on sector-based emission controls in Delhi, for developing a mitigation strategy addressing both pollutants.

In this study, we demonstrate the value of such a framework for supporting decision makers in determining better mitigation strategies. We give examples of its use in investigating impacts of mitigation scenarios on $PM_{2.5}$ and O_3 pollutions in Delhi, and demonstrate that

regional joint coordination of emission controls over National Capital Region (NCR) of Delhi is essential for an effective reduction of $PM_{2.5}$ whilst minimizing the risk of O_3 increase.

2. Materials and Methods

2.1 WRF-Chem Model Baseline Simulation

WRF-Chem (v3.9.1) – an online, fully coupled chemistry transport model (Grell et al., 2005) – has been widely used in previous studies of air quality across India (Marrapu et al., 2014;Mohan and Gupta, 2018;Gupta and Mohan, 2015;Mohan and Bhati, 2011). The model has also been used to estimate the health burden (Conibear et al., 2018;Ghude et al., 2016) and reduction in crop yields (Ghude et al., 2014) from the exposure to $PM_{2.5}$ and O_3 over India.

In this study, we focus on the hot and dry pre-monsoon period in Delhi, when average temperatures are around 32 ^oC and relative humidity (RH) is about 35% (Ojha et al., 2012). O_3 approaches its annual peak in pre-monsoon due to strong solar radiation (Ghude et al., 2008;Ojha et al., 2012). During the pre-monsoon period, desert dust can contribute significantly to particulate matter in Delhi (Kumar et al., 2014b;Kumar et al., 2014a). Here, we perform WRF-Chem simulation for the period of 2–15 May 2015 (with two additional days for spin-up), ~~which~~ when Delhi was not significantly influenced by dust storms ~~in Delhi~~ according to MODIS observations (https://earthdata.nasa.gov/earth-observation-data/near-real-time/hazards-and-disasters/dust-storms). Strong dust storms started to influence the Indo Gangetic Plain on 21-24 April and 19 May 2015, respectively. This minimizes the uncertainties resulting from dust storm simulation and permits a stronger focus on anthropogenic emissions. Resuspended dust from road traffic is also a major contributor to $PM_{2.5}$ in Delhi, and this is estimated and included in the emission inventory as described below.

The model configuration follows the study of Marrapu et al. (2014), and the parameterizations used are listed in Table 1. Three nested domains are used, with coverage of South Asia (45 km resolution), the Indo Gangetic Plain (15 km resolution), and the National Capital Region (5 km resolution), see Fig. 1. A test simulation with a fourth domain over Delhi at 1.67 km resolution suggests that a further increase in resolution does not substantially improve model performance (details in Text S1), and this is in line with results from a previous study (Mohan and Bhati, 2011). The Carbon Bond Mechanism version Z (CBMZ, Zaveri and Peters, 1999) coupled with the MOSAIC (Zaveri et al., 2008) aerosol module with four size bins is used to represent gaseous chemical reaction and aerosol chemical and dynamical processes. We neglect wet scavenging and cloud chemistry processes here, as the impact of these is likely to be negligible during the dry pre-monsoon period over India. No precipitation was recoded in Delhi during the simulation period.

The initial and boundary conditions for chemical species are provided from MOZART-4 global results (https://www.acom.ucar.edu/wrf-chem/mozart.shtml). Our baseline simulation is driven by European Centre for Medium-Range Weather Forecasts (ECMWF) meteorological data, as we find that this reproduces regional meteorology better than that from the National Centers for Environmental Prediction (NCEP) over India, consistent with a recent study (Chatani and Sharma, 2018). The ECMWF reanalysis dataset (ERA-Interim) assimilates observations with a number of nearly 10^7 per day (Dee et al., 2011), and is ~~provides analysis data~~used for grid nudging, initial and boundary conditions for WRF-Chem ~~with~~at horizontal and temporal resolutions of $0.75^o \times 0.75^o$ and 6 hours, respectively. The wind pattern and temperature over Delhi in May 2015 is generally captured well in simulations driven by either meteorological dataset, but the model captures the variation in relative humidity much better (R=0.7) with ECMWF data than with NCEP data (R=0.4, negative bias of 20-40%). More detailed discussion is provided in Text S2.

The high-resolution Fire Inventory from NCAR (FINN, Wiedinmyer et al., 2011) is adopted to provide biomass burning emissions. Interactive biogenic emissions are included using the Model of Emissions of Gases and Aerosols from Nature (MEGAN, Guenther et al., 2006). The global Emission Database for Global Atmospheric Research with Task Force on Hemispheric Transport of Air Pollution (EDGAR-HTAP, Janssens-Maenhout et al., 2015) version 2.2 (year 2010) at 0.1° × 0.1° resolution is used to represent anthropogenic emissions apart from over Delhi, where they are represented by a high-resolution monthly inventory for 2015 developed under the System of Air Quality Forecasting and Research (SAFAR) project (Sahu et al., 2011;Sahu et al., 2015). In the absence of a diurnal variation in emissions specific to Delhi, we adopt diurnal variations from Europe in this study (Denier van der Gon et al., 2011). The SAFAR inventory provides emission fluxes of PM_{10}, $PM_{2.5}$, black carbon, organic carbon, NOx, CO, SO_2 and NMVOC (non-methane volatile organic compounds) from five sectors, including power (POW), industry (IND), domestic or residential (DOM), traffic (TRA) and wind blow dust from roads (WBD). Wind blow dust includes dust resuspended from vehicle movement on paved and unpaved roads (Sahu et al., 2011), and is therefore closely related to traffic emissions, and we combine this into the traffic sector for our study.

The NMVOC emissions are speciated according to the EDGAR (v4.3.2) global inventory (Huang et al., 2017), and are then lumped for the CBMZ chemistry scheme. The speciation mapping is detailed in Table 2 and described below, and a toolkit has been developed to perform this mapping. Emissions of alcohols and ethers are split 20%:80% between methanol and ethanol by mass and then converted to molar emissions with a fractionation based on Murrells et al. (2009). Emissions of paraffin carbon (PAR) are calculated by converting mass emissions from each VOC group to molar emissions and then multiplying by the number of paraffin carbons in order to conserve carbon. Hexanes and higher alkanes are converted to molar emissions of hexane and then multiplied by six to give PAR emissions. Other alkenes

are mapped to molar emissions of butane, and this is then apportioned between terminal olefin carbons (OLET), internal olefin carbons (OLEI) and PAR on a molar ratio of 1:1:4 following (Zaveri and Peters, 1999). Ketones are split 60%:40% by mass between acetone (KET) and methyl-ethyl ketone (MEK), then converted to molar emissions with fractions based on (Murrells et al., 2009). As MEK is not included in the CBMZ mechanism, we apportion molar emissions of MEK equally between KET and PAR.

2.2 Observational Network

Air quality and meteorological monitoring networks are operated in Delhi under the SAFAR project coordinated by IITM (Ministry of Earth Sciences, Government of India). Measurements of $PM_{2.5}$, O_3 and NOx during the May 2015 simulation period are available from six monitoring stations in Delhi: C V Raman (CVR), Delhi University (DEU), Indira Ghandi International Airport Terminal-3 (AIR), Ayanagar (AYA), NCMRWF (NCM) and Pusa (PUS). The instruments are calibrated and measurements are quality controlled in the SAFAR project (http://safar.tropmet.res.in); more details are given in previous studies (Sahu et al., 2011;Beig et al., 2013;Aslam et al., 2017). Site locations are shown in Fig. 2 and measured variables are given in Table S1.

2.3 Global Sensitivity Analysis of Urban Air Pollution

We perform global sensitivity analysis (GSA) (Iooss and Lemaître, 2015) to quantify the sensitivity of modelled outputs ($PM_{2.5}$ and O_3 for this study) to changes in the model inputs, which for this study are emissions ~~of~~from the different ~~each~~ emission sectors. One-at-a-time sensitivity analysis is a common way of calculating model sensitivity and involves ~~where~~varying a single model input~~s is varied~~ while the other inputs are fixed at nominal values, e.g., Wild (2007). While one-at-a-time approach is ~~a~~ relatively easy ~~method~~ to implement, it assumes that the~~independence of~~ model response to different inputs is independent and this can

lead to biased results ~~of the sensitivity~~ (Saltelli et al., 1999;Pisoni et al., 2018;Carslaw et al., 2013). ~~Global sensitivity analysis (GSA) has major advantages over a simple one-at-a-time sensitivity analysis, where a single input is varied while the other inputs are fixed at nominal values, as the latter approach can lead to underestimation of the true sensitivity.~~ GSA overcomes the problems of the one-at-a-time approach by averaging over the other inputs rather than fixing them at specific values. This allows calculation of first-order sensitivity indices (SIs) for each variable, corresponding to the i^{th} input variable and the j^{th} output point, is given by the Eq. 1 (Ryan et al., 2018).

$$SI_{i,j} = \frac{Var[E(y_j \mid x_i)]}{Var(y_j)} \times 100\% \quad (1)$$

where x_i is the i^{th} element of the input; and y_j is the j^{th} element of the output. The 'E(•)' and 'Var(•)' denote the mathematical function that calculate the expectation and variance, respectively. The simplest way of computing $SI_{i,j}$ is by brute force, but this is also the most computationally intensive (Ryan et al., 2018).

The extended Fourier Amplitude Sensitivity Test (eFAST), first developed by Saltelli et al. (1999), is a commonly used approach to perform GSA and calculate SIs~~,~~ and is adopted in this study because of its high efficiency. A basic overview and detailed equations of the eFAST method ~~See~~are given in the section 2.2.2 of~~in~~ Ryan et al. (2018) ~~for~~. A challenge to using ~~Since~~ eFAST ~~for performing GSA~~ is that it typically requires thousands of model runs. To overcome this,~~,~~ we employ a computationally cheaper surrogate model in place of our expensive simulation model WRF-Chem. A surrogate model is a simple~~refers to any~~ model (usually statistical ~~model~~) which can map the inputs to the outputs of the simulation~~another~~ model with sufficiently good accuracy given the same inputs. In this study, we choose a type of surrogate model called a ~~use~~ Gaussian process emulator, which works like a function for multi-

dimensional interpolation and has been used extensively in many areas of applied science (Carslaw et al., 2013;Koehler and Owen, 1996;Queipo et al., 2005;Vanuytrecht and Willems, 2014;vu et al., 2015;Degroote et al., 2012) and uncertainty assessment of atmospheric models (Lee et al., 2016;Lee et al., 2012;Lee et al., 2011).~~ion to create the surrogate model~~ ~~And a~~ Gaussian process emulators typically require~~s~~ a relatively small number of runs of the computational-expensive model to generate; ~~T~~this is in contrast to other surrogate modelling approaches, such as neural networks, which typically require thousands of model runs to train them. For a basic overview of a Gaussian process emulator see O'Hagan (2006), detailed introduction and equations are also given in the section 2.3 of Ryan et al. (2018).~~, since a Gaussian process emulator typically requires a relatively small number of runs of the computationally expensive model to generate. This is in contrast to other surrogate modelling approaches, such as neural networks, which typically require thousands of model runs to train them. Gaussian process emulators have been used previously in the uncertainty assessment of atmospheric models.~~ Before using the emulator in place of the WRF-Chem model~~simulator~~ to carry out the thousands of model runs required for ~~the~~ GSA, we ~~need to~~ train the emulator using a relatively small number of ~~executions of the~~ WRF-Chem model runs ~~simulator~~. Following previous~~these~~ studies (Carslaw et al., 2013;Lee et al., 2016), a Maximin Latin hypercube space-filling design ~~approach~~ is employed to ~~provide~~ select the designs of training runs for WRF-Chem. ~~.~~ Latin hypercube sampling is a statistical method for generating a near-random sample of parameter values from a multidimensional distribution (Shields and Zhang, 2016). Here, we search through 100,000 Latin hypercube random designs to find the optimal one where the parameter space is filled most effectively. This ensures that the sets of inputs chosen cover~~are~~ as large a fraction of ~~space filling in~~ the input space as possible. Full details (including R codes) of how to generate the Gaussian process emulator, eFAST method and GSA can be found in~~More details of these approaches are described in a previous study~~ Ryan et al. (2018).

In this study, we focus on a limited number of the emission sectors to demonstrate the effectiveness of the approach: domestic/residential emissions in Delhi (DOM), traffic emissions in Delhi (TRA, including WBD), power and industry in Delhi (POW+IND) and total emissions in the National Capital Region outside Delhi (NCR). NCR represents the contribution of regional transport to pollution in Delhi. According to the SAFAR emission inventory, the total $PM_{2.5}$ emissions of DOM, TRA, POW+IND and NCR are about 1.8, 6.1, 3.1 and 8.5 Gg/month in May 2015, respectively. The Gaussian process emulators is trained usingare built based on 20 executions training runs of the WRF-Chem simulation model, with emission scaling drawn from a variation range of 0-200% for each of the four specified sectors (Table S2). Emulation of the impacts of mitigation scenarios on $PM_{2.5}$ and O_3 can be performed in minutes on a laptop, in contrast to simulations with WRF-Chem which require a few days on a high-performance computing cluster. The accuracy of the emulator as a surrogate of WRF-Chem simulatormodel is evaluated was performed using aWe perform 'leave-one-out' cross-validation (Bastos and O'Hagan, 2009). This involves training the emulator using 19 out of the 20 sets of inputs/outputs from the WRF-Chem simulation model runs and then evaluatingrunning the emulator againstat the 20th simulationset of inputs. The resulting emulator outputs are then compared with the outputs from WRF-Chem. This process is carried out for each of the 20 sets of inputs/outputs. Given that the output space is multi-dimensional (i.e. modelled O_3 and $PM_{2.5}$ varied spatially and in time), the validation of the emulator by comparing 10,000 (random-samples varied spatially and in time) of emulator output values withagainst the corresponding output values of the WRF-Chem model. Theis emulator validation plot is shown in Fig. 3. Modelled and emulated O_3 and $PM_{2.5}$ lie very close to the 1:1 line with R^2 values of more than 95% as shown in Fig. 3, indicating that the emulation provides an accurate representation of the input-output relationship of the WRF-Chem model.

~~with 10,000 random samples to check that the Gaussian process emulator can fully represent the results of WRF-Chem. Modelled and emulated O_3 and $PM_{2.5}$ lie very close to the 1:1 line with R values of more than 0.99 as shown in Fig. 3, suggesting that the emulation provides a good representation of the model.~~

2.4 Response Surfaces

Response surfaces are useful for investigating the relationship between model inputs and outputs, in this case between sectoral emissions and modelled pollutant concentrations. They have been widely applied for air quality studies and policy making (EPA, 2006b, a;Zhao et al., 2017;Xing et al., 2017). Here, we analyse the responses of $PM_{2.5}$ and O_3 to changes in emissions from each sector of between 0% and 200%. The computationally efficient Gaussian process emulation enables us to generate response surfaces without the computational burden of a large number of runs of the WRF-chem model.

2.5 Outline of Analysis

We use the WRF-Chem model to simulate the hourly concentrations of O_3 and $PM_{2.5}$ over the Delhi region during 2-15 May 2015 and evaluate the results against observations. We perform a simple sensitivity analysis to investigate the contributions of biomass burning and biogenic emissions to $PM_{2.5}$ and O_3 in Delhi. We then conduct a global sensitivity analysis, using the eFAST method (see section 2.3) along with Gaussian process emulation, to determine the sensitivity of modelled O_3 and $PM_{2.5}$ concentrations to changes in the dominant anthropogenic emission sectors. Finally, we generate response surfaces to identify appropriate mitigation strategies for reducing $PM_{2.5}$ while minimizing the risks from O_3 increase.

3. Results and Discussion

3.1 Model Performance

The WRF-Chem model captures the general magnitude and variation in $PM_{2.5}$ well (Fig. 4a), with mean bias and error of about -3.5% and 11%, respectively, and an index of agreement (Willmott et al., 2012) of 75%. The frequency distributions of modelled $PM_{2.5}$ are also similar to the observations, with differences in mean and median concentrations of less than 10%, although high concentration spikes are missed by the model (Fig. S1). The modelled $PM_{2.5}$ peaks around 09:00 local time (LT) because the rush hour enhances traffic emissions before the planetary boundary layer (PBL) height has increased (Fig. 4a). This is also seen in the modelled results at DEU (Fig. S2), which is closer to a motorway and shows a more intense $PM_{2.5}$ peak in the morning rush hour. $PM_{2.5}$ is overestimated during the morning rush hour (around 09:00 am) and underestimated during the early morning (03:00-05:00 LT, Fig. 4a and Fig. S2). This may suggest that there is an earlier rush hour or more traffic activity at night in Delhi than in European cities, since we adopted European diurnal emission patterns in this study in the absence of local information. Detailed studies of traffic emissions and their variation in Delhi would help improve these model simulations.

The modelled chemical composition of $PM_{2.5}$ is shown in Fig. S3. Secondary inorganic aerosol (SIA), including sulphate, nitrate and ammonium, only contributes ~25% of aerosol mass in our simulation. In the absence of particle inorganic composition measurements during the simulation period, we compare our results with a previous modelling study of Delhi during the post-monsoon season (Marrapu et al., 2014), which also shows a ~25% contribution of SIA to $PM_{2.5}$ loading, in line with our results. Furthermore, our results are also consistent with an observational study, which reported the mass fraction of organic matter (usually calculated as 1.4 times OC) and elemental carbon (usually equivalent to black carbon in modelling studies, Chen et al., 2016b) in $PM_{2.5}$ of ~20% and ~6% in Delhi during May 2015, respectively (Sharma et al., 2018).

The model well captures the peak O_3 with a bias of less than 5%, although it underestimates O_3 during night-time (Fig. 4b). In general, the diurnal pattern and magnitude of O_3 are captured by WRF-Chem (Fig. 4b), with normalized mean bias and error of about -20% and 35%, respectively, and an index of agreement of 65%. The underestimation during night-time is likely to be because NOx is overestimated by a factor of 2-3 at night (Fig. S4), and the excess NO depletes O_3. This is indicated by the frequency distribution of O_3 and NOx (Fig. S5), where the median values of observed O_3 and NOx are matched well by the model. However, the higher peaks of modelled NOx concentration lower the modelled O_3 levels, indicating that Delhi is in VOC-limited photochemical regime. Similar results are found at AYA (Fig. S6). The larger underestimation of O_3 at NCM (Fig. S5d, industrial environment site) suggests that NOx emission from the industry sector may be overestimated.

3.2 Impacts of Biogenic and Biomass Burning Emissions

Before exploring the importance of the four selected anthropogenic emission sectors on $PM_{2.5}$ and O_3 in Delhi during simulation period, we investigate the contributions from other factors (biomass burning and biogenic emissions). We ~~remove~~ turn off these sources in the WRF-Chem simulation and find that there is a negligible contribution from biogenic emissions to $PM_{2.5}$ concentrations over Delhi in this season (Fig. 4c and 4d). It is worth noting that biogenic emissions may contribute to secondary organic aerosol (SOA) in Delhi, but the formation of SOA is not ~~well~~ represented well by the CBMZ-MOSAIC chemistry-aerosol mechanisms used in this study. However, this weakness is not expected to have a major influence on our pre-monsoon results; as described ~~before~~above, the difference of organic matter fraction between simulation and observation (Sharma et al., 2018) in May 2015 is less than 5%. About 10% of $PM_{2.5}$ in Delhi is derived from biomass burning during the simulation period. Crop burning in Haryana and Punjab states is a major source of this (Jethva et al., 2018;Cusworth et al., 2018). In contrast, there is a negligible contribution from biomass

burning to O_3. However, there is a 15-20% contribution to O_3 from biogenic emission of VOCs, highlighting that O_3 production in Delhi is strongly VOC-limited.

3.3 Effect of the Diurnal Variation in Emissions

In order to investigate the competing influences of meteorology and human activities on the diurnal patterns of $PM_{2.5}$ and O_3 over Delhi, we test the effect of removing the diurnal variation in anthropogenic emissions ('noDiurnal', see Fig. 4c and 4d). Modelled $PM_{2.5}$ concentrations are very similar to the 'baseline' run during daytime when the PBL is well developed, with differences of less than 5%. This suggests that meteorological processes such as vertical mixing, advection and transport are the dominant factors controlling $PM_{2.5}$ in the daytime. In contrast, freshly emitted pollutants are trapped at night when the PBL is shallow, and concentrations are very sensitive to the emission flux, so that the diurnal pattern of emissions is the dominant factor at night. The $PM_{2.5}$ concentration is almost doubled in the early morning (03:00-09:00 LT, Fig. 4c) when the PBL is shallow and emissions in the 'noDiurnal' case are higher. There is also a large increase in NOx in the early morning (Fig. S4), which leads to greater depletion of O_3 (Fig. 4d). However, the concentration of O_3 is about 20-25% higher during the ozone peak hour in the afternoon in the 'noDiurnal' case, as the daytime NOx emissions are less (Fig. S4). This sensitivity test also highlights the VOC-limited nature of O_3 production in Delhi.

3.4 Sensitivity Analysis of Pollutants in Delhi

The importance of each anthropogenic emission sector to pollutant concentrations in Delhi is investigated using global sensitivity analysis and indicated by global sensitivity indices (SIs), as shown in Fig. 5. The sensitivity index is a measure of the contribution of the variation in pollutants from one emission sector to the total variation across all four sectors considered here.

A larger SI indicates a larger influence from the corresponding sector to the modelled average surface $PM_{2.5}$ or O_3 over Delhi City Region (marked in Fig. 2) in this study.

The $PM_{2.5}$ concentration is most sensitive to emissions from the NCR region surrounding Delhi, with a sensitivity index higher than 50% most of time (Fig. 5a) and reaching 80-90% and ~60% during 03:00-07:00 LT and 12:00-17:00 LT, respectively. During the rush hours in the morning and evening, the sensitivity to NCR emissions is lower, while the sensitivity to Delhi traffic emissions increases by ~30%. Around 10:00 LT, local traffic emissions and emissions from NCR have a similar effect on $PM_{2.5}$. In contrast, local traffic emissions dominate the $PM_{2.5}$ in Delhi around 20:00 LT, with a sensitivity contribution of up to ~80%. This is caused by the collapse of the PBL in the evening rush hour at around 20:00 LT which enhances the sensitivity to fresh local emissions. Local traffic emissions contribute ~60% of primary $PM_{2.5}$ emission in Delhi (Fig. 6a), which remains concentrated in the PBL during rush hours. In contrast, the fully developed PBL in the daytime mixes air down from the free troposphere (Chen et al., 2016a), where regional transport of pollutants from NCR can be important. This could explain the second peak in the sensitivity to NCR emissions (50-60%) during the afternoon (Fig. 5a).

The variation of O_3 in Delhi City Region is overwhelmingly dominated by local traffic emissions with a sensitivity index higher than 80% at night-time (Fig. 5b), whenre O_3 and traffic emissions are anti-correlated. Traffic contributes ~75% of total NOx emission in Delhi (Fig. 6b), and the shallow PBL during the night traps the NOx. This removes O_3 through chemical reaction in the absence of solar radiation. As the PBL develops in the morning, the sensitivity of O_3 to traffic decreases and the sensitivity to NCR emissions increases. The sensitivity to NCR emissions reaches its highest point (70%) when the PBL is fully developed around 15:00 LT. As discussed above, the downward mixing of air from the free troposphere

and dilution of local emissions in the fully developed PBL could be the reason for this. The O_3 peak coincides with the highest PBL at this time because photolysis and development of the PBL are both driven by solar radiation. The development of the PBL increases the contribution from regional transport, and precursors emitted from the NCR are one of the dominant contributors to the peak of O_3 in Delhi. The NOx, mainly originatinged from traffic emissions, is underestimated by ~30% during the O_3 peak period (Fig. S4). This uncertainty can propagate into the Gaussian process emulator and could lead to underestimation of trafficthe influence of traffic on peak O_3, peak to some extent. Bbut, it is not expected to change theo nature of our conclusion about the predominance of regional transport and local traffic emissions. In addition, it is noteworthy that the NOx-rich urban plume from Delhi has a substantial influence on O_3 in downwind regions across the NCR as well, as discussed in Text S3.

3.5 Mitigation Strategies

To demonstrate a framework for developing better mitigation strategies for addressing both $PM_{2.5}$ and O_3 pollution in Delhi, emission-sector based pollutant response surfaces are generated using Gaussian process emulation (Fig. 7). For local emissions in Delhi, we focus mainly on traffic and residential sectors here, because we find that power and industrial emissions have a more limited influence on $PM_{2.5}$ and O_3 concentrations in Delhi (Fig. 5). A range of different mitigation strategies are analysed, aiming at mitigating $PM_{2.5}$ pollution whilst minimizing the risk of O_3 increase.

We find that the responses of $PM_{2.5}$ and O_3 to each emission sector are nearly linear in Delhi. The response surfaces show that reducing local traffic emissions in Delhi leads to an efficient decrease in $PM_{2.5}$ loading (Fig. 7a) but increases O_3 greatly (Fig. 7b). Reducing local domestic emissions decreases $PM_{2.5}$ loading less than reducing traffic but without increasing O_3. The small impact on O_3 may be because domestic emissions are not a major source of NOx,

contributing only 15% of that from traffic (Fig. 6). A 10-20% reduction in NOx is expected when reduce local domestic emissions by 50%; ~~while,~~but a 35-45% reduction ~~in NOx can be expected by~~ is seen for a 50% reduction in local traffic emissions (Fig. S7). In addition, VOC is reduced more than NOx when controlling domestic emissions, as the VOC/NOx emission ratio (kg/kg) is 1.8 in contrast to a ratio of 0.4 for traffic emissions. Greater reduction of VOC suppresses the increase of O_3 in Delhi, which is a VOC-limited environment. A reduction in local traffic emissions alone of 50% could decrease Delhi $PM_{2.5}$ loading by 15-20%, but this would also increase O_3 by 20-25%. We note that our model may underestimate the influence of traffic emissions on O_3 to some extent as described above (section 3.4), suggesting that the ozone increase could be stronger than we predict. ~~-~~To prevent the side-effect of increasing O_3 by controls on traffic emissions, regional cooperation would be required to reduce emissions in the NCR region surrounding Delhi by 25-30%, which also permits a further reduction of $PM_{2.5}$ by 5-10% (Fig. 7c and 7d). This is consistent with a recent study showing that ~60% of $PM_{2.5}$ in Delhi originates from outside (Amann et al., 2017)~~-~~. We test this by performing an additional run with WRF-Chem using emission reductions of 50% and 30% for sectors of local traffic and the surrounding NCR region, respectively. We compare the WRF-Chem results of the additional run and the base case (without change of emissions) against the corresponding results from Gaussian process emulator (Fig. S8~~13~~). We find that the $PM_{2.5}$ and O_3 results from the model runs lie within 5% of those estimated with the emulator and with R^2 higher than 95%, demonstrating the high quality of the emulation approach adopted here and underlining its deeper value for identifying mitigation approaches. The suggested regional joint mitigation with NCR surrounding Delhi is in line with a recent study for mitigating $PM_{2.5}$ in Beijing, which showed that regional coordination over the North China Plain could lead to a reduction in $PM_{2.5}$ of up to 40% in winter (Liu et al., 2016).

4. Summary

Previous studies have shown that emission controls focusing on mitigation of $PM_{2.5}$ may result in substantial increases of surface ozone over urban areas that are in VOC-limited photochemical environment. Comprehensive studies of mitigation strategies with respect to both $PM_{2.5}$ and O_3 are urgently required, but are limited in India. In this study, we demonstrate a numerical framework for informing emission-sector based mitigation strategies in Delhi that account for multiple pollutants.

By using Gaussian process emulation with an air quality model (WRF-Chem), we generate a computational efficient surrogate model for performing global sensitivity analysis and calculating emission-sector based pollutant response surfaces. These enable us to exhaustively investigate the impacts of different mitigation scenarios on $PM_{2.5}$ and O_3 in Delhi, which help decision makers choose better mitigation strategies. Global sensitivity analysis shows that pollutants originating from the National Capital Region (NCR) surrounding Delhi and local traffic emissions are the major contributors of $PM_{2.5}$ and O_3 in Delhi. They co-dominate the O_3 peak and $PM_{2.5}$ in Delhi during daytime, while the regional transport governs $PM_{2.5}$ during the night, in line with a recent study showing that ~60% of $PM_{2.5}$ in Delhi originates from outside (Amann et al., 2017). Controlling local traffic emissions in Delhi would have the notable side effect of increasing O_3 ~~increases~~, at least in the pre-monsoon/summer period (peak O_3 season) that we consider here. This is in line with ~~the~~ recent increases in~~of~~ O_3 seen in China (Silver et al., 2018;Li et al., 2018). The Chinese experience suggests that regional joint coordination is required to~~for~~ effectively mitigate PM2.5 pollution in Beijing (Liu et al., 2016). Our pollutant response surfaces go one step further and suggest that joint coordinated emission controls with the NCR region surrounding Delhi would be required to not only achieve a more ambitious reduction of $PM_{2.5}$ but also to minimize the risk of O_3 increases ~~and to achieve a more ambitious~~

~~reduction of $PM_{2.5}$~~. In the regional joint coordination, residential energy use could be a dominant emission sector over a large region in India (Conibear et al., 2018).

5. Discussion

The experiences of developed countries (Dooley, 2002;EPA, 2011) and recently in China (Huang et al., 2018a;Wang et al., 2019) show that regional joint coordination can be achieved by changing energy infrastructure (e.g., replacing fossil fuel by renewable energy and natural gas), desulphurisation and denitrification technologies, popularization of new energy vehicles, strict control of vehicle exhaust and reducing road and construction dust. Further studies with more detailed information on specific emission sectors and strategies for clean-technology development and popularization would permit deeper insight into air pollution mitigation approaches suitable for Delhi. These are needed to address both $PM_{2.5}$ which has a higher impact on public health (e.g., Huang et al., 2018a), and O_3 which greatly impacts regional ecology and agriculture (e.g., Avnery et al., 2011). A more comprehensive evaluation of the health and economic benefits of different mitigation strategies would greatly help Indian decision makers, and the framework we have demonstrated here would provide a strong foundation for this.

Author contributions

O. W. and Y. C. conceived the study. Y. C. performed the simulations and emulation, and processed and interpreted the results with help from Y. W. E. R. designed and built the Gaussian Process emulator. G. B. and S. K. S. provided the observations and SAFAR emission inventory. D. L., A. A., S. A. N. and G. M. help pre-process the emission data and develop the emission toolkit. V. S. and R. S. S. provided useful discussion on the emission inventory. R. S. S. led the development of the PROMOTE project. Y. C. and O. W. wrote the manuscript with inputs from all co-authors.

Notes

The authors declare no competing financial interest.

Acknowledgments

This work was supported by the NERC/MOES/Newton Fund supported PROMOTE project (grant number NE/P016405/1 and NE/P016480/1). The work of E. Ryan was supported by the NERC (grant number NE/N003411/1). The Indian Institute of Tropical Meteorology, Pune, is supported by the Ministry of Earth Science, Government of India. The observations and high-resolution emission inventory are provided by the SAFAR project under MoES (http://safar.tropmet.res.in). The authors appreciate the efforts of the entire team involved in PROMOTE and SAFAR projects. The paper is based on interpretation of scientific results and in no way reflect the viewpoint of the funding agency.

Data availability

NCEP FNL operational model global tropospheric analyses (ds083.2) were downloaded from https://rda.ucar.edu/data/ds083.2/, and sea surface temperature data were downloaded from http://polar.ncep.noaa.gov/sst/. ECMWF interim reanalyses (ERA-Interim) were downloaded from http://apps.ecmwf.int/datasets/data/interim-full-daily. MOZART-4 global model results are downloaded from http://www.acd.ucar.edu/wrf-chem/mozart.shtml. FINN biomass burning emissions dataset is downloaded from http://bai.acom.ucar.edu/Data/fire/. Toolkits for emission processing are available from https://github.com/douglowe/WRF_UoM_EMIT/releases/tag/v1.0 and https://github.com/douglowe/PROMOTE-emissions/releases/tag/v1.0 .

References:

Amann, M., Bertok, I., Borken-Kleefeld, J., Cofala, J., Heyes, C., Höglund-Isaksson, L., Klimont, Z., Nguyen, B., Posch, M., Rafaj, P., Sandler, R., Schöpp, W., Wagner, F., and Winiwarter, W.: Cost-effective control of air quality and greenhouse gases in Europe: Modeling and policy applications, Environmental Modelling & Software, 26, 1489-1501, https://doi.org/10.1016/j.envsoft.2011.07.012, 2011.

Amann, M., Purohit, P., Bhanarkar, A. D., Bertok, I., Borken-Kleefeld, J., Cofala, J., Heyes, C., Kiesewetter, G., Klimont, Z., Liu, J., Majumdar, D., Nguyen, B., Rafaj, P., Rao, P. S., Sander, R., Schöpp, W., Srivastava, A., and Vardhan, B. H.: Managing future air quality in megacities: A case study for Delhi, Atmospheric Environment, 161, 99-111, https://doi.org/10.1016/j.atmosenv.2017.04.041, 2017.

Ashworth, K., Wild, O., and Hewitt, C. N.: Impacts of biofuel cultivation on mortality and crop yields, Nature Clim. Change, 3, 492-496, 10.1038/nclimate1788, 2013.

Aslam, M. Y., Krishna, K. R., Beig, G., Tinmaker, M. I. R., and Chate, D. M.: Seasonal Variation of Urban Heat Island and Its Impact on Air-Quality Using SAFAR Observations at Delhi, India, American Journal of Climate Change, Vol.06No.02, 12, 10.4236/ajcc.2017.62015, 2017.

Avnery, S., Mauzerall, D. L., Liu, J., and Horowitz, L. W.: Global crop yield reductions due to surface ozone exposure: 2. Year 2030 potential crop production losses and economic damage under two scenarios of O3 pollution, Atmospheric Environment, 45, 2297-2309, https://doi.org/10.1016/j.atmosenv.2011.01.002, 2011.

Bastos, L. S., and O'Hagan, A.: Diagnostics for Gaussian Process Emulators, Technometrics, 51, 425-438, 10.1198/TECH.2009.08019, 2009.

Beig, G., Chate, D. M., Ghude, S. D., Ali, K., Satpute, T., Sahu, S. K., Parkhi, N., and Trimbake, H. K.: Evaluating population exposure to environmental pollutants during Deepavali fireworks displays using air quality measurements of the SAFAR network, Chemosphere, 92, 116-124, http://dx.doi.org/10.1016/j.chemosphere.2013.02.043, 2013.

Carslaw, K. S., Lee, L. A., Reddington, C. L., Pringle, K. J., Rap, A., Forster, P. M., Mann, G. W., Spracklen, D. V., Woodhouse, M. T., Regayre, L. A., and Pierce, J. R.: Large contribution of natural aerosols to uncertainty in indirect forcing, Nature, 503, 67, 10.1038/nature12674, 2013.

Chatani, S., and Sharma, S.: Uncertainties Caused by Major Meteorological Analysis Data Sets in Simulating Air Quality Over India, Journal of Geophysical Research: Atmospheres, 123, 6230-6247, doi:10.1029/2017JD027502, 2018.

Chen, L., Guo, B., Huang, J., He, J., Wang, H., Zhang, S., and Chen, S. X.: Assessing air-quality in Beijing-Tianjin-Hebei region: The method and mixed tales of PM2.5 and O3, Atmospheric Environment, https://doi.org/10.1016/j.atmosenv.2018.08.047, 2018.

Chen, Y., Cheng, Y., Ma, N., Wolke, R., Nordmann, S., Schüttauf, S., Ran, L., Wehner, B., Birmili, W., van der Gon, H. A. C. D., Mu, Q., Barthel, S., Spindler, G., Stieger, B., Müller, K., Zheng, G. J., Pöschl, U., Su, H., and Wiedensohler, A.: Sea salt emission, transport and influence on size-segregated nitrate simulation: a case study in northwestern Europe by WRF-Chem, Atmos. Chem. Phys., 16, 12081-12097, 10.5194/acp-16-12081-2016, 2016a.

Chen, Y., Cheng, Y. F., Nordmann, S., Birmili, W., Denier van der Gon, H. A. C., Ma, N., Wolke, R., Wehner, B., Sun, J., Spindler, G., Mu, Q., Pöschl, U., Su, H., and Wiedensohler, A.: Evaluation of the size segregation of elemental carbon (EC) emission in Europe: influence on the simulation of EC long-range transportation, Atmos. Chem. Phys., 16, 1823-1835, 10.5194/acp-16-1823-2016, 2016b.

Chen Y, Wild O., Conibear L., Ran L., He J., Wang L., Wang Y.: Local Characteristics of and Exposure to Fine Particulate Matter (PM2.5) in Four Indian Megacities, Atmospheric Environment, 10.1016/j.aeaoa.2019.100052, 2019

Chowdhury, S., and Dey, S.: Cause-specific premature death from ambient PM2.5 exposure in India: Estimate adjusted for baseline mortality, Environment International, 91, 283-290, https://doi.org/10.1016/j.envint.2016.03.004, 2016.

Chowdhury, S., Dey, S., Tripathi, S. N., Beig, G., Mishra, A. K., and Sharma, S.: "Traffic intervention" policy fails to mitigate air pollution in megacity Delhi, Environmental Science & Policy, 74, 8-13, http://dx.doi.org/10.1016/j.envsci.2017.04.018, 2017.

Conibear, L., Butt, E. W., Knote, C., Arnold, S. R., and Spracklen, D. V.: Residential energy use emissions dominate health impacts from exposure to ambient particulate matter in India, Nature Communications, 9, 617, 10.1038/s41467-018-02986-7, 2018.

Cusworth, D. H., Mickley, L. J., Sulprizio, M. P., Liu, T., Marlier, M. E., DeFries, R. S., Guttikunda, S. K., and Gupta, P.: Quantifying the influence of agricultural fires in northwest India on urban air pollution in Delhi, India, Environmental Research Letters, 13, 044018, 10.1088/1748-9326/aab303, 2018.

Dee, D. P., Uppala, S. M., Simmons, A. J., Berrisford, P., Poli, P., Kobayashi, S., Andrae, U., Balmaseda, M. A., Balsamo, G., Bauer, P., Bechtold, P., Beljaars, A. C. M., van de Berg, L., Bidlot, J., Bormann, N., Delsol,

C., Dragani, R., Fuentes, M., Geer, A. J., Haimberger, L., Healy, S. B., Hersbach, H., Hólm, E. V., Isaksen, L., Kållberg, P., Köhler, M., Matricardi, M., McNally, A. P., Monge-Sanz, B. M., Morcrette, J.-J., Park, B.-K., Peubey, C., de Rosnay, P., Tavolato, C., Thépaut, J.-N., and Vitart, F.: The ERA-Interim reanalysis: configuration and performance of the data assimilation system, Quarterly Journal of the Royal Meteorological Society, 137, 553-597, 10.1002/qj.828, 2011.

Degroote, J., Couckuyt, I., Vierendeels, J., Segers, P., and Dhaene, T.: Inverse modelling of an aneurysm's stiffness using surrogate-based optimization and fluid-structure interaction simulations, Structural and Multidisciplinary Optimization, 46, 457-469, 10.1007/s00158-011-0751-7, 2012.

Denier van der Gon, H. A. C., Hendriks, C., Kuenen, J., Segers, A., and Visschedijk, A.: TNO Report: Description of current temporal emission patterns and sensitivity of predicted AQ for temporal emission patterns 2011.

Dooley, E.: Clearing the Air over the London Fog, Environmental Health Perspectives, 110, A748-A749, 2002.

Duncan, B. N., Lamsal, L. N., Thompson, A. M., Yoshida, Y., Lu, Z., Streets, D. G., Hurwitz, M. M., and Pickering, K. E.: A space-based, high-resolution view of notable changes in urban NOx pollution around the world (2005–2014), Journal of Geophysical Research: Atmospheres, 121, 976-996, doi:10.1002/2015JD024121, 2016.

EPA: Technical support document for the proposed mobile source air toxics rule: ozone modeling, Office of Air Quality Planning and Standards, US Environmental Protection Agency, Research Triangle Park, NC, US, 49, (last access: 01 Oct. 2018), 2006a.

EPA: Technical support document for the proposed PM NAAQS rule: Response Surface Modeling, Office of Air Quality Planning and Standards, US Environmental Protection Agency, Research Triangle Park, NC, US, 48, (lase access: 01 Oct. 2018), 2006b.

EPA: Benefits and costs of the Clean Air Act 1990-2020, the second prospective study, https://www.epa.gov/clean-air-act-overview/benefitsand-costs-clean-air-act-1990-2020-second-prospective-study, (last access: 20 Aug. 2018). 2011.

Fleming, Z. L., Doherty, R. M., Von Schneidemesser, E., Malley, C. S., Cooper, O. R., Pinto, J. P., Colette, A., Xu, X., Simpson, D., Schultz, M. G., Lefohn, A. S., Hamad, S., Moolla, R., Solberg, S., and Feng, Z.: Tropospheric Ozone Assessment Report: Present-day ozone distribution and trends relevant to human health, Elem Sci. Anth, 6, 12, 2018.

Gao, M., Guttikunda, S. K., Carmichael, G. R., Wang, Y., Liu, Z., Stanier, C. O., Saide, P. E., and Yu, M.: Health impacts and economic losses assessment of the 2013 severe haze event in Beijing area, Science of The Total Environment, 511, 553-561, https://doi.org/10.1016/j.scitotenv.2015.01.005, 2015.

Gao, M., Beig, G., Song, S., Zhang, H., Hu, J., Ying, Q., Liang, F., Liu, Y., Wang, H., Lu, X., Zhu, T., Carmichael, G. R., Nielsen, C. P., and McElroy, M. B.: The impact of power generation emissions on ambient PM2.5 pollution and human health in China and India, Environment International, 121, 250-259, https://doi.org/10.1016/j.envint.2018.09.015, 2018.

Gao, M., Sherman, P., Song, S., Yu, Y., Wu, Z., and McElroy, M. B.: Seasonal prediction of Indian wintertime aerosol pollution using the ocean memory effect, Science Advances, 5, eaav4157, 10.1126/sciadv.aav4157, 2019.

Ghude, S. D., Jain, S. L., Arya, B. C., Beig, G., Ahammed, Y. N., Kumar, A., and Tyagi, B.: Ozone in ambient air at a tropical megacity, Delhi: characteristics, trends and cumulative ozone exposure indices, J Atmos Chem, 60, 237-252, 10.1007/s10874-009-9119-4, 2008.

Ghude, S. D., Jena, C., Chate, D. M., Beig, G., Pfister, G. G., Kumar, R., and Ramanathan, V.: Reductions in India's crop yield due to ozone, Geophysical Research Letters, 41, 5685-5691, 10.1002/2014GL060930, 2014.

Ghude, S. D., Chate, D. M., Jena, C., Beig, G., Kumar, R., Barth, M. C., Pfister, G. G., Fadnavis, S., and Pithani, P.: Premature mortality in India due to PM2.5 and ozone exposure, Geophysical Research Letters, 43, 4650-4658, 10.1002/2016GL068949, 2016.

Grell, G. A., Peckham, S. E., Schmitz, R., McKeen, S. A., Frost, G., Skamarock, W. C., and Eder, B.: Fully coupled "online" chemistry within the WRF model, Atmospheric Environment, 39, 6957-6975, http://dx.doi.org/10.1016/j.atmosenv.2005.04.027, 2005.

Guenther, A., Karl, T., Harley, P., Wiedinmyer, C., Palmer, P. I., and Geron, C.: Estimates of global terrestrial isoprene emissions using MEGAN (Model of Emissions of Gases and Aerosols from Nature), Atmos. Chem. Phys., 6, 3181-3210, 10.5194/acp-6-3181-2006, 2006.

Gupta, M., and Mohan, M.: Validation of WRF/Chem model and sensitivity of chemical mechanisms to ozone simulation over megacity Delhi, Atmospheric Environment, 122, 220-229, http://dx.doi.org/10.1016/j.atmosenv.2015.09.039, 2015.

Hollaway, M., Wild, O., Yang, T., Sun, Y., Xu, W., Xie, C., Whalley, L., Slater, E., Heard, D., and Liu, D.: Photochemical impacts of haze pollution in an urban environment, Atmos. Chem. Phys. Discuss., 2019, 1-26, 10.5194/acp-2019-29, 2019.

Huang, G., Brook, R., Crippa, M., Janssens-Maenhout, G., Schieberle, C., Dore, C., Guizzardi, D., Muntean, M., Schaaf, E., and Friedrich, R.: Speciation of anthropogenic emissions of non-methane volatile organic compounds: a global gridded data set for 1970–2012, Atmos. Chem. Phys., 17, 7683-7701, 10.5194/acp-17-7683-2017, 2017.

Huang, J., Pan, X., Guo, X., and Li, G.: Health impact of China's Air Pollution Prevention and Control Action Plan: an analysis of national air quality monitoring and mortality data, The Lancet Planetary Health, 2, e313-e323, 10.1016/S2542-5196(18)30141-4, 2018a.

Huang, X., Wang, Z., and Ding, A.: Impact of Aerosol-PBL Interaction on Haze Pollution: Multiyear Observational Evidences in North China, Geophysical Research Letters, 45, 8596-8603, 10.1029/2018GL079239, 2018b.

Iooss, B., and Lemaître, P.: A review on global sensitivity analysis methods. In: Meloni, C., Dellino, G. (Eds.), Uncertainty Management in Simulationoptimization of Complex Systems: Algorithms and Applications. Springer, 2015.

Janssens-Maenhout, G., Crippa, M., Guizzardi, D., Dentener, F., Muntean, M., Pouliot, G., Keating, T., Zhang, Q., Kurokawa, J., Wankmüller, R., Denier van der Gon, H., Kuenen, J. J. P., Klimont, Z., Frost, G., Darras, S., Koffi, B., and Li, M.: HTAP_v2.2: a mosaic of regional and global emission grid maps for 2008 and 2010 to study hemispheric transport of air pollution, Atmos. Chem. Phys., 15, 11411-11432, 10.5194/acp-15-11411-2015, 2015.

Jethva, H., Chand, D., Torres, O., Gupta, P., Lyapustin, A., and Patadia, F.: Agricultural Burning and Air Quality over Northern India: A Synergistic Analysis using NASA’s A-train Satellite Data and Ground Measurements, Aerosol and Air Quality Research, 18, 1756-1773, 10.4209/aaqr.2017.12.0583, 2018.

Khare, M., Gargava, P., and Khan, A. A.: Effect of PM2.5 chemical constituents on atmospheric visibility impairment AU - Khanna, Isha, Journal of the Air & Waste Management Association, 68, 430-437, 10.1080/10962247.2018.1425772, 2018.

Koehler, J. R., and Owen, A. B.: 9 Computer experiments, in: Handbook of Statistics, Elsevier, 261-308, 1996.

Kumar, R., Barth, M. C., Madronich, S., Naja, M., Carmichael, G. R., Pfister, G. G., Knote, C., Brasseur, G. P., Ojha, N., and Sarangi, T.: Effects of dust aerosols on tropospheric chemistry during a typical pre-monsoon season dust storm in northern India, Atmos. Chem. Phys., 14, 6813-6834, 10.5194/acp-14-6813-2014, 2014a.

Kumar, R., Barth, M. C., Pfister, G. G., Naja, M., and Brasseur, G. P.: WRF-Chem simulations of a typical pre-monsoon dust storm in northern India: influences on aerosol optical properties and radiation budget, Atmos. Chem. Phys., 14, 2431-2446, 10.5194/acp-14-2431-2014, 2014b.

Kumar, R., Barth, M. C., Pfister, G. G., Delle Monache, L., Lamarque, J. F., Archer-Nicholls, S., Tilmes, S., Ghude, S. D., Wiedinmyer, C., Naja, M., and Walters, S.: How Will Air Quality Change in South Asia by 2050?, Journal of Geophysical Research: Atmospheres, 123, 1840-1864, doi:10.1002/2017JD027357, 2018.

Lee, L. A., Carslaw, K. S., Pringle, K. J., Mann, G. W., and Spracklen, D. V.: Emulation of a complex global aerosol model to quantify sensitivity to uncertain parameters, Atmos. Chem. Phys., 11, 12253-12273, 10.5194/acp-11-12253-2011, 2011.

Lee, L. A., Carslaw, K. S., Pringle, K. J., and Mann, G. W.: Mapping the uncertainty in global CCN using emulation, Atmos. Chem. Phys., 12, 9739-9751, 10.5194/acp-12-9739-2012, 2012.

Lee, L. A., Reddington, C. L., and Carslaw, K. S.: On the relationship between aerosol model uncertainty and radiative forcing uncertainty, Proceedings of the National Academy of Sciences, 113, 5820-5827, 10.1073/pnas.1507050113, 2016.

Lelieveld, J., Bourtsoukidis, E., Brühl, C., Fischer, H., Fuchs, H., Harder, H., Hofzumahaus, A., Holland, F., Marno, D., Neumaier, M., Pozzer, A., Schlager, H., Williams, J., Zahn, A., and Ziereis, H.: The South Asian monsoon—Pollution pump and purifier, Science, 10.1126/science.aar2501, 2018.

Li, K., Jacob, D. J., Liao, H., Shen, L., Zhang, Q., and Bates, K. H.: Anthropogenic drivers of 2013–2017 trends in summer surface ozone in China, Proceedings of the National Academy of Sciences, 201812168, 10.1073/pnas.1812168116, 2018.

Liu, H., Wang, X. M., Pang, J. M., and He, K. B.: Feasibility and difficulties of China's new air quality standard compliance: PRD case of PM_{2.5} and ozone from 2010 to 2025, Atmos. Chem. Phys., 13, 12013-12027, 10.5194/acp-13-12013-2013, 2013.

Liu, J., Mauzerall, D. L., Chen, Q., Zhang, Q., Song, Y., Peng, W., Klimont, Z., Qiu, X., Zhang, S., Hu, M., Lin, W., Smith, K. R., and Zhu, T.: Air pollutant emissions from Chinese households: A major and underappreciated ambient pollution source, Proceedings of the National Academy of Sciences, 113, 7756-7761, 10.1073/pnas.1604537113, 2016.

Liu, J., Xiang, S., Yi, K., and Tao, W.: Co-Mitigation of Ozone and PM2.5 Pollution over the Beijing-Tianjin-Hebei Region, 2017 AGU Fall Meeting, New Orleans, 2017AGUFM.A53F2327L, 2017.

Lu, X., Hong, J., Zhang, L., Cooper, O. R., Schultz, M. G., Xu, X., Wang, T., Gao, M., Zhao, Y., and Zhang, Y.: Severe Surface Ozone Pollution in China: A Global Perspective, Environmental Science & Technology Letters, 10.1021/acs.estlett.8b00366, 2018.

Marrapu, P., Cheng, Y., Beig, G., Sahu, S., Srinivas, R., and Carmichael, G. R.: Air quality in Delhi during the Commonwealth Games, Atmos. Chem. Phys., 14, 10619-10630, 10.5194/acp-14-10619-2014, 2014.

Menon, S., Hansen, J., Nazarenko, L., and Luo, Y.: Climate Effects of Black Carbon Aerosols in China and India, Science, 297, 2250-2253, 10.1126/science.1075159, 2002.

Mohan, M., and Bhati, S.: Analysis of WRF Model Performance over Subtropical Region of Delhi, India, Advances in Meteorology, 2011, 10.1155/2011/621235, 2011.

Mohan, M., and Gupta, M.: Sensitivity of PBL parameterizations on PM10 and ozone simulation using chemical transport model WRF-Chem over a sub-tropical urban airshed in India, Atmospheric Environment, 185, 53-63, https://doi.org/10.1016/j.atmosenv.2018.04.054, 2018.

Mukherjee, A., and Toohey, D. W.: A study of aerosol properties based on observations of particulate matter from the U.S. Embassy in Beijing, China, Earth's Future, 4, 381-395, doi:10.1002/2016EF000367, 2016.

Murrells, T. P., Passant, N. R., Thistlethwaite, G., Wagner, A., Li, Y., Bush, T., Norris, J., Walker, C., Stewart, R. A., Tsagatakis, I., Whiting, R., Conolly, C., Okamura, S., Peirce, M., Sneddon, S., Webb, J., Thomas, J., MacCarthy, J., Choudrie, S., Webb, N., and Mould, R.: UK Emissions of Air Pollutants 1970 to 2009, Available: https://uk-air.defra.gov.uk/assets/documents/reports/cat07/1401131501_NAEI_Annual_Report_2009.pdf, (last access: 12 Nov. 2018), 2009.

O'Hagan, A.: Bayesian analysis of computer code outputs: A tutorial, Reliability Engineering & System Safety, 91, 1290-1300, https://doi.org/10.1016/j.ress.2005.11.025, 2006.

O'Hagan, A., and West, M.: Handbook of applied Bayesian analysis, Oxford University Press, New York, 2009.

Ojha, N., Naja, M., Singh, K. P., Sarangi, T., Kumar, R., Lal, S., Lawrence, M. G., Butler, T. M., and Chandola, H. C.: Variabilities in ozone at a semi-urban site in the Indo-Gangetic Plain region: Association with the meteorology and regional processes, Journal of Geophysical Research: Atmospheres, 117, doi:10.1029/2012JD017716, 2012.

Pisoni, E., Clappier, A., Degraeuwe, B., and Thunis, P.: Adding spatial flexibility to source-receptor relationships for air quality modeling, Environmental Modelling & Software, 90, 68-77, https://doi.org/10.1016/j.envsoft.2017.01.001, 2017.

Pisoni, E., Albrecht, D., Mara, T. A., Rosati, R., Tarantola, S., and Thunis, P.: Application of uncertainty and sensitivity analysis to the air quality SHERPA modelling tool, Atmospheric Environment, 183, 84-93, https://doi.org/10.1016/j.atmosenv.2018.04.006, 2018.

Pope, C. A., Ezzati, M., and Dockery, D. W.: Fine-Particulate Air Pollution and Life Expectancy in the United States, New England Journal of Medicine, 360, 376-386, 10.1056/NEJMsa0805646, 2009.

Queipo, N. V., Haftka, R. T., Shyy, W., Goel, T., Vaidyanathan, R., and Kevin Tucker, P.: Surrogate-based analysis and optimization, Progress in Aerospace Sciences, 41, 1-28, https://doi.org/10.1016/j.paerosci.2005.02.001, 2005.

Ran, L., Zhao, C., Geng, F., Tie, X., Tang, X., Peng, L., Zhou, G., Yu, Q., Xu, J., and Guenther, A.: Ozone photochemical production in urban Shanghai, China: Analysis based on ground level observations, Journal of Geophysical Research: Atmospheres, 114, D15301, 10.1029/2008JD010752, 2009.

Ryan, E., Wild, O., Voulgarakis, A., and Lee, L.: Fast sensitivity analysis methods for computationally expensive models with multi-dimensional output, Geosci. Model Dev., 11, 3131-3146, 10.5194/gmd-11-3131-2018, 2018.

Sahu, S. K., Beig, G., and Parkhi, N. S.: Emissions inventory of anthropogenic PM2.5 and PM10 in Delhi during Commonwealth Games 2010, Atmospheric Environment, 45, 6180-6190, http://dx.doi.org/10.1016/j.atmosenv.2011.08.014, 2011.

Sahu, S. K., Beig, G., and Parkhi, N.: High Resolution Emission Inventory of NOx and CO for Mega City Delhi, India, Aerosol and Air Quality Research, 15, 1137-1144, 10.4209/aaqr.2014.07.0132, 2015.

Saltelli, A., Tarantola, S., and Chan, K. P. S.: A Quantitative Model-Independent Method for Global Sensitivity Analysis of Model Output, Technometrics, 41, 39-56, 10.1080/00401706.1999.10485594, 1999.

Sharma, A., Ojha, N., Pozzer, A., Mar, K. A., Beig, G., Lelieveld, J., and Gunthe, S. S.: WRF-Chem simulated surface ozone over south Asia during the pre-monsoon: effects of emission inventories and chemical mechanisms, Atmos. Chem. Phys., 17, 14393-14413, 10.5194/acp-17-14393-2017, 2017.

Sharma, S. K., Mandal, T. K., Sharma, A., Jain, S., and Saraswati: Carbonaceous Species of PM2.5 in Megacity Delhi, India During 2012–2016, Bulletin of Environmental Contamination and Toxicology, 100, 695-701, 10.1007/s00128-018-2313-9, 2018.

Shields, M. D., and Zhang, J.: The generalization of Latin hypercube sampling, Reliability Engineering & System Safety, 148, 96-108, https://doi.org/10.1016/j.ress.2015.12.002, 2016.

Silver, B., Reddington, C. L., Arnold, S. R., and Spracklen, D. V.: Substantial changes in air pollution across China during 2015–2017, Environmental Research Letters, 13, 114012, 10.1088/1748-9326/aae718, 2018.

Stafoggia, M., Bellander, T., Bucci, S., Davoli, M., de Hoogh, K., de' Donato, F., Gariazzo, C., Lyapustin, A., Michelozzi, P., Renzi, M., Scortichini, M., Shtein, A., Viegi, G., Kloog, I., and Schwartz, J.: Estimation of daily PM10 and PM2.5 concentrations in Italy, 2013–2015, using a spatiotemporal land-use random-forest model, Environment International, 124, 170-179, https://doi.org/10.1016/j.envint.2019.01.016, 2019.

Thunis, P., Degraeuwe, B., Pisoni, E., Ferrari, F., and Clappier, A.: On the design and assessment of regional air quality plans: The SHERPA approach, Journal of Environmental Management, 183, 952-958, https://doi.org/10.1016/j.jenvman.2016.09.049, 2016.

Turner, M. C., Jerrett, M., Pope, C. A., 3rd, Krewski, D., Gapstur, S. M., Diver, W. R., Beckerman, B. S., Marshall, J. D., Su, J., Crouse, D. L., and Burnett, R. T.: Long-Term Ozone Exposure and Mortality in a Large Prospective Study, American journal of respiratory and critical care medicine, 193, 1134-1142, 10.1164/rccm.201508-1633OC, 2016.

Vanuytrecht, E., and Willems, P.: Global sensitivity analysis of yield output from the water productivity model, Environmental Modelling and Software, 51, 323-332, 10.1016/j.envsoft.2013.10.017, 2014.

vu, N., Rafiee, R., Zhuang, X., Lahmer, T., and Rabczuk, T.: Uncertainty quantification for multiscale modeling of polymer nanocomposites with correlated parameters, Composites Part B: Engineering, 68, 446-464, 10.1016/j.compositesb.2014.09.008, 2015.

Wang, T., Xue, L., Brimblecombe, P., Lam, Y. F., Li, L., and Zhang, L.: Ozone pollution in China: A review of concentrations, meteorological influences, chemical precursors, and effects, Science of The Total Environment, 575, 1582-1596, https://doi.org/10.1016/j.scitotenv.2016.10.081, 2017.

Wang, Y., and Chen, Y.: Significant Climate Impact of Highly Hygroscopic Atmospheric Aerosols in Delhi, India, Geophysical Research Letters, 0, 10.1029/2019GL082339, 2019.

Wang, Y., Li, W., Gao, W., Liu, Z., Tian, S., Shen, R., Ji, D., Wang, S., Wang, L., Tang, G., Song, T., Cheng, M., Wang, G., Gong, Z., Hao, J., and Zhang, Y.: Trends in particulate matter and its chemical compositions in China from 2013–2017, Science China Earth Sciences, 10.1007/s11430-018-9373-1, 2019.

WHO: Review of evidence on health aspects of air pollution - REVIHAAP final technical report, World Health Organization: Geneva, 2013.

WHO: Neurological syndrome and congenital anomalies, Zika Situation Report, 1-7, 2016a.

WHO: WHO Global Urban Ambient Air Pollution Database (update 2016), Available: http://www.who.int/airpollution/data/cities-2016/en/,, (last access: 08 Nov. 2018), 2016b.

Wiedinmyer, C., Akagi, S. K., Yokelson, R. J., Emmons, L. K., Al-Saadi, J. A., Orlando, J. J., and Soja, A. J.: The Fire INventory from NCAR (FINN): a high resolution global model to estimate the emissions from open burning, Geosci. Model Dev., 4, 625-641, 10.5194/gmd-4-625-2011, 2011.

Wild, O.: Modelling the global tropospheric ozone budget: exploring the variability in current models, Atmos. Chem. Phys., 7, 2643-2660, 10.5194/acp-7-2643-2007, 2007.

Willmott, C. J., Robeson, S. M., and Matsuura, K.: A refined index of model performance, International Journal of Climatology, 32, 2088-2094, doi:10.1002/joc.2419, 2012.

Wu, J., Xu, Y., and Zhang, B.: Projection of PM2.5 and Ozone Concentration Changes over the Jing-Jin-Ji Region in China, 143-146 pp., 2015.

Xing, J., Wang, S., Zhao, B., Wu, W., Ding, D., Jang, C., Zhu, Y., Chang, X., Wang, J., Zhang, F., and Hao, J.: Quantifying Nonlinear Multiregional Contributions to Ozone and Fine Particles Using an Updated Response Surface Modeling Technique, Environmental Science & Technology, 51, 11788-11798, 10.1021/acs.est.7b01975, 2017.

Xing, J., Ding, D., Wang, S., Zhao, B., Jang, C., Wu, W., Zhang, F., Zhu, Y., and Hao, J.: Quantification of the enhanced effectiveness of NOx control from simultaneous reductions of VOC and NH3 for reducing air pollution in the Beijing–Tianjin–Hebei region, China, Atmos. Chem. Phys., 18, 7799-7814, 10.5194/acp-18-7799-2018, 2018.

Zaveri, R. A., and Peters, L. K.: A new lumped structure photochemical mechanism for large-scale applications, J. Geophys. Res., 104, 30387-30415, 1999.

Zaveri, R. A., Easter, R. C., Fast, J. D., and Peters, L. K.: Model for Simulating Aerosol Interactions and Chemistry (MOSAIC), Journal of Geophysical Research: Atmospheres, 113, 10.1029/2007JD008782, 2008.

Zhao, B., Wu, W., Wang, S., Xing, J., Chang, X., Liou, K. N., Jiang, J. H., Gu, Y., Jang, C., Fu, J. S., Zhu, Y., Wang, J., Lin, Y., and Hao, J.: A modeling study of the nonlinear response of fine particles to air pollutant emissions in the Beijing–Tianjin–Hebei region, Atmos. Chem. Phys., 17, 12031-12050, 10.5194/acp-17-12031-2017, 2017.

Table 1. Configuration of WRF-Chem

Physics	**WRF option**
Micro physics	Lin scheme (Lin, 1983)
Surface Layer	MM5 similarity
Boundary layer	YSU (Hong, 2006)
Cumulus	Grell 3D
Urban	3-category UCM
Shortwave radiation	Goddard shortwave (Chou, 1998)
Longwave radiation	Rapid Radiative Transfer Model
Chemistry and Aerosol	**Chem option**
Gas-phase mechanism	CBMZ (Zaveri and Peters, 1999)
Aerosol module	MOSAIC with 4 bins (~40 nm to 10 μm) (Zaveri et al., 2008)
Photolysis rate	Fast-J photolysis scheme (Wild et al., 2000)
Emissions Inventories	
Anthropogenic Emissions	SAFAR-2015 Delhi and EDGAR-HTAP v2.2
Biogenic Emissions	MEGAN (Guenther et al., 2006)
Biomass Burning Emissions	FINN (Wiedinmyer et al., 2011)

Table 2. Map of NMVOC from EDGAR emission to CBMZ scheme.

EDGAR Name	**Description**	**CBMZ [mol]**
VOC1	Alcohols	20% CH_3OH
		80% C_2H_5OH
VOC2	Ethane	C_2H_6
VOC3	Propane	PAR*3
VOC4	Butane	PAR*4
VOC5	Pentane	PAR*5
VOC6	Hexanes + other Alkanes	PAR*6
VOC7	Ethene	ETH
VOC8	Propene	OLET+PAR
VOC9	Ethyne	PAR*2
VOC10	Isoprene	ISOP
VOC11	Monoterpenes	ISOP*2
VOC12	Other Alkenes	OLEI*0.5+OLET*0.5+PAR*2
VOC13	Benzene	TOL-PAR
VOC14	Toluene	TOL
VOC15	Xylenes	XYL
VOC16	Trimethylbenzenes	XYL+PAR
VOC17	Other Aromatics	XYL+PAR
VOC18	Esters	RCOOH
VOC19	Ethers	20% CH_3OH
		80% C_2H_5OH
VOC21	Formaldehyde	HCHO
VOC22	Other Aldehydes	ALD2
VOC23	Ketones	60% KET
		40% KET+PAR
VOC24	Alkanoic Acids	RCOOH

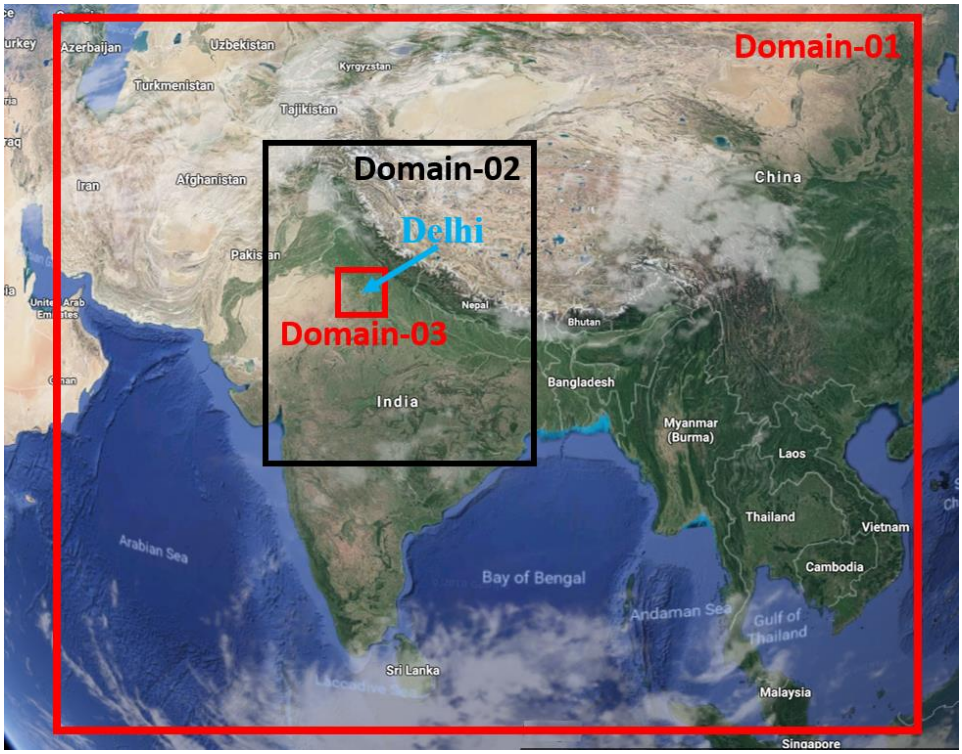

Figure 1. Map of simulation domains, modified from Google Earth.

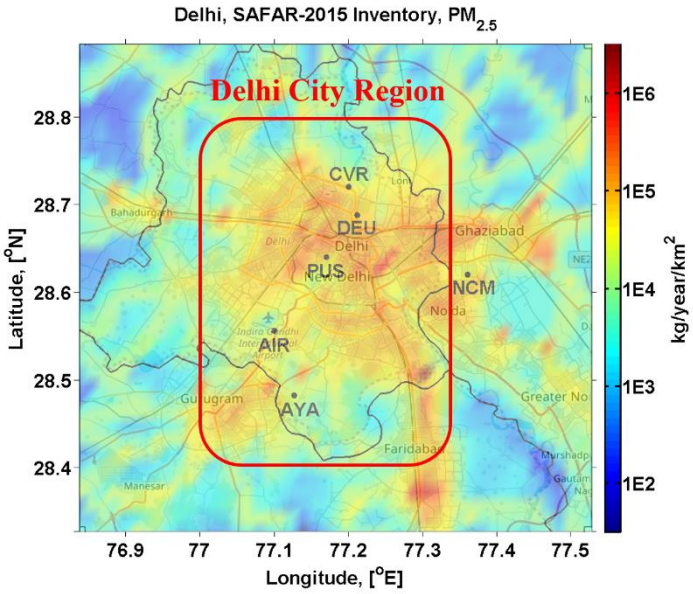

Figure 2. SAFAR inventory of total $PM_{2.5}$ emission. The locations of measurement sites over Delhi are marked by black dots, and the Delhi City Region is marked by a red box.

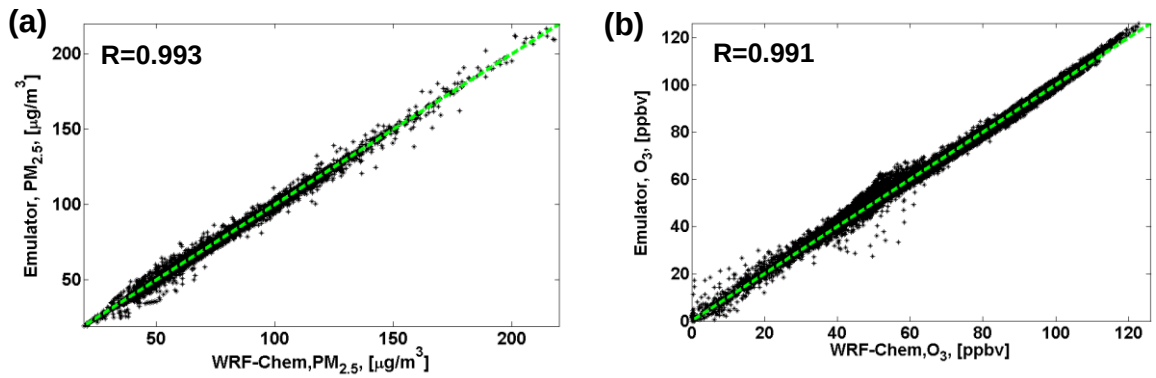

Figure 3. Validation of Gaussian process emulator with WRF-Chem model. (**a**) $PM_{2.5}$; (**b**) O_3. The green dashed line indicates the 1:1 line.

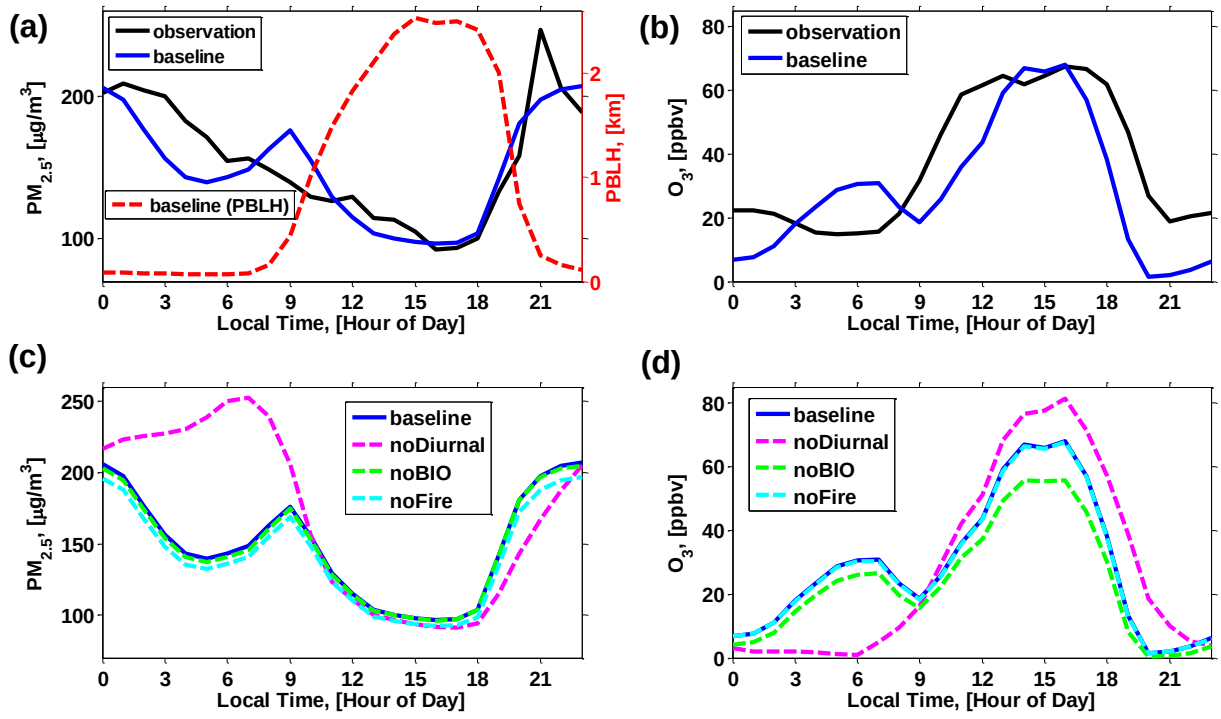

Figure 4. Average diurnal patterns of pollutants during the 2-15 May 2015 simulation period. (**a**) Modelled and observed $PM_{2.5}$ and model PBL height (PBLH); (**b**) O_3; (**c**) results of sensitivity studies for $PM_{2.5}$; (**d**) results of sensitivity studies for O_3. The left panels (a, c) are for site CVR, and the right panels (b, d) are for site AIR (marked in Fig. 2). The sensitivity runs 'noFire' and 'noBIO' show model results without biomass burning and biogenic emissions, respectively; and 'noDiurnal' show model results with constant anthropogenic emissions rates throughout the day.

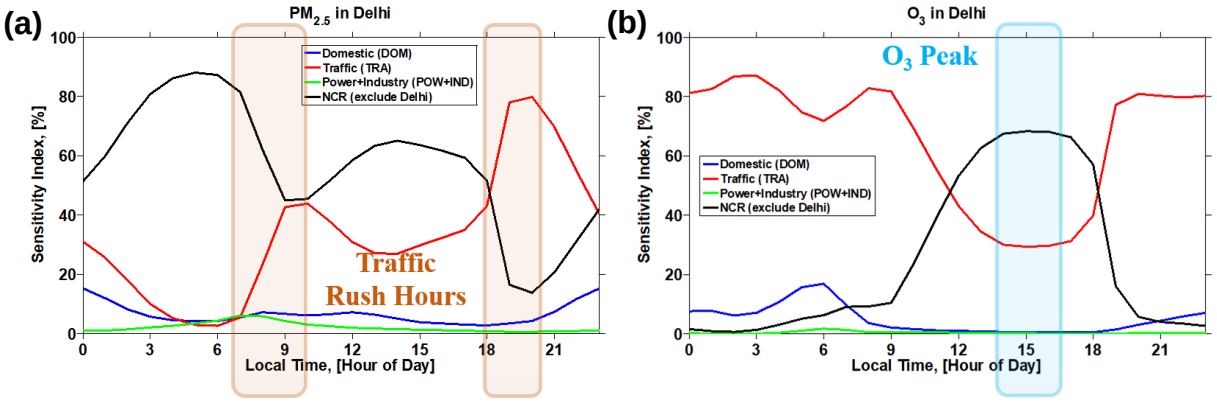

Figure 5. Averaged diurnal pattern of global sensitivity indices during the 2-15 May simulation period. (**a**) $PM_{2.5}$; (**b**) O_3. The $PM_{2.5}$ and O_3 results are averaged over Delhi City Region (marked with red box in Fig. 2). The morning and evening rush hours and the period of peak ozone are marked with the boxes to highlight the notable changes in contribution from each emission sector.

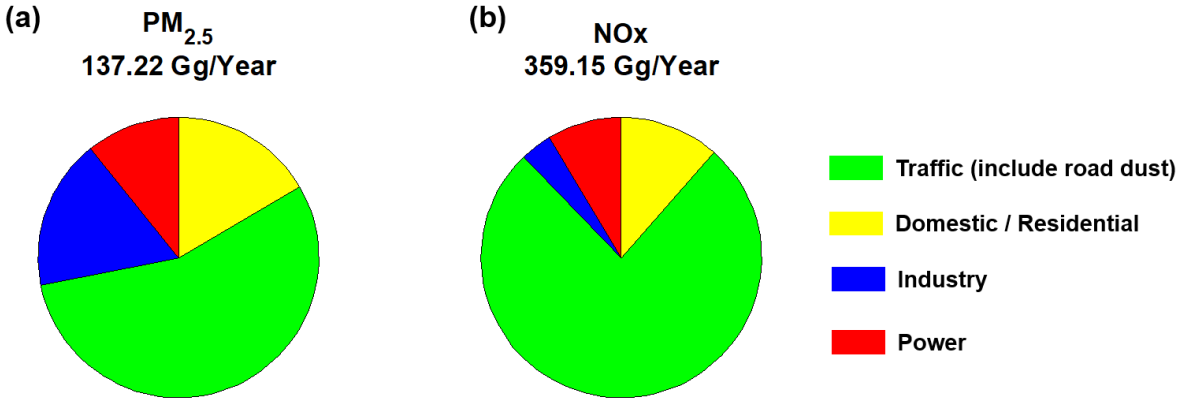

Figure 6. Annual emission of different sectors in Delhi from SAFAR inventory. (a) PM2.5; (b) NOx. The emissions of black carbon, organic carbon, non-methane VOC (NMVOC) and SO_2 are given in the supplementary Fig. S132.

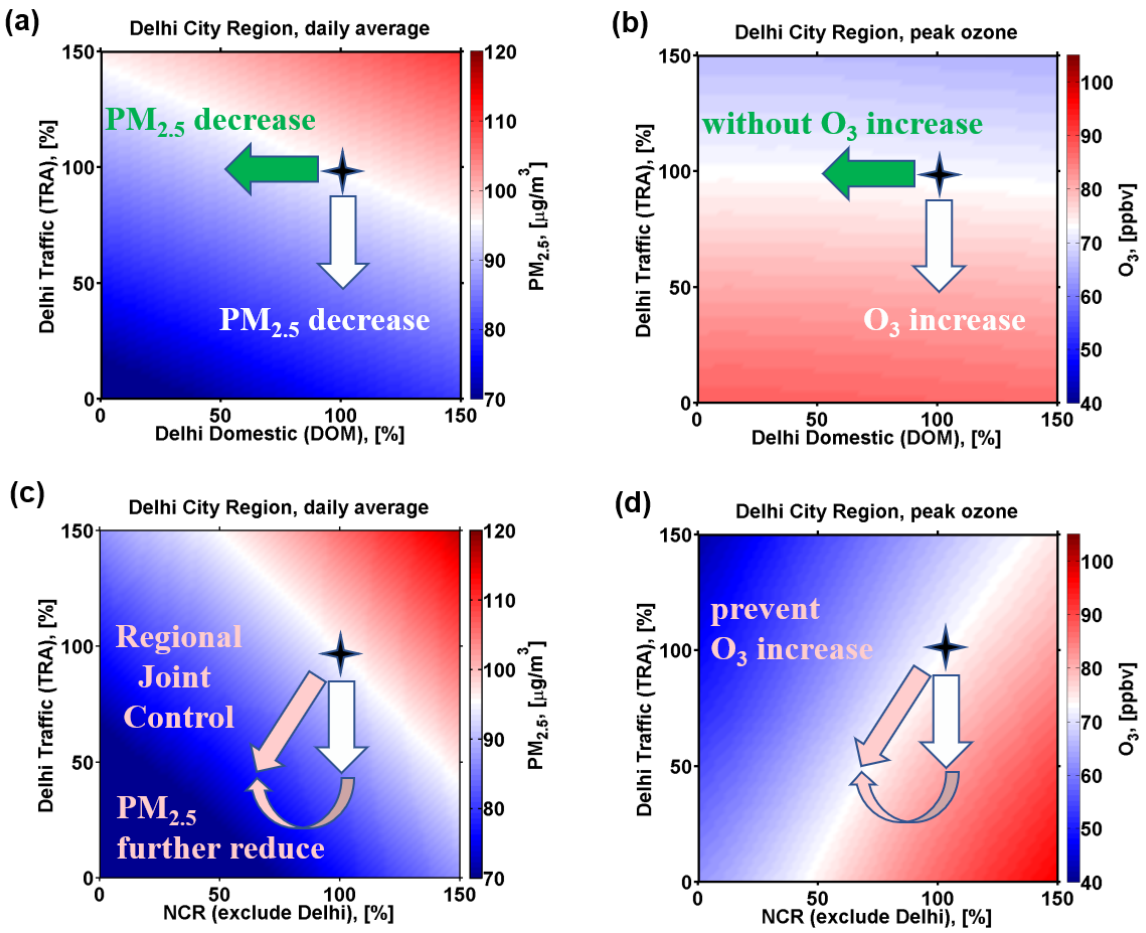

Figure 7. Response surfaces for $PM_{2.5}$ and ozone concentrations over Delhi City Region, averaged over 2-15 May 2018. (**a**) Daily average of $PM_{2.5}$ concentrations as a function of local traffic and domestic emissions in Delhi; (**b**) peak hourly ozone concentrations as a function of local traffic and domestic emissions in Delhi; (**c**) daily average of $PM_{2.5}$ concentrations as a function of local traffic emissions in Delhi and emissions in NCR region surrounding Delhi; and (**d**) peak hourly ozone concentrations as a function of local traffic emissions in Delhi and emissions in NCR region surrounding Delhi. The star indicates current conditions and the arrows show the effect of possible emission controls.

References:

Chou, M., Suarez, M., Ho, C., Yan, M., and Lee, K.: Parameterizations for Cloud Overlapping and Shortwave Single-Scattering Properties for Use in General Circulation and Cloud Ensemble, Models, J. Climate, 11, 202-214, 1998.

Guenther, A., Karl, T., Harley, P., Wiedinmyer, C., Palmer, P. I., and Geron, C.: Estimates of global terrestrial isoprene emissions using MEGAN (Model of Emissions of Gases and Aerosols from Nature), Atmos. Chem. Phys., 6, 3181-3210, 10.5194/acp-6-3181-2006, 2006.

Hong, S.-Y., Noh, Y., and Dudhia, J.: A new vertical diffusion package with an explicit treatment of entrainment processes, Mon. Weather Rev., 134, 2318-2341, 2006.

Lin, Y., Farley, R., and Orville, H.: Bulk Parameterization of the Snow Field in a Cloud Model, J. Clim. Appl. Meteorol., 22, 1065-1092, 1983.

Wiedinmyer, C., Akagi, S. K., Yokelson, R. J., Emmons, L. K., Al-Saadi, J. A., Orlando, J. J., and Soja, A. J.: The Fire INventory from NCAR (FINN): a high resolution global model to estimate the emissions from open burning, Geosci. Model Dev., 4, 625-641, 10.5194/gmd-4-625-2011, 2011.

Wild, O., Zhu, X., and Prather, M. J.: Fast-J: Accurate Simulation of In- and Below-Cloud Photolysis in Tropospheric Chemical Models, J. Atmos. Chem., 37, 245-282, 2000.

Zaveri, R. A., and Peters, L. K.: A new lumped structure photochemical mechanism for large-scale applications, J. Geophys. Res., 104, 30387-30415, 1999.

Zaveri, R. A., Easter, R. C., Fast, J. D., and Peters, L. K.: Model for Simulating Aerosol Interactions and Chemistry (MOSAIC), Journal of Geophysical Research: Atmospheres, 113, 10.1029/2007JD008782, 2008.

Supporting Information

for

Mitigation of $PM_{2.5}$ and Ozone Pollution in Delhi: A Sensitivity Study during the Pre-monsoon period

Ying Chen[1,2*], Oliver Wild[1,2], Edmund Ryan[1,9], Saroj Kumar Sahu[4], Douglas Lowe[5], Scott Archer-Nicholls[6], Yu Wang[5], Gordon McFiggans[5], Tabish Ansari[1], Vikas Singh[7], Ranjeet Sokhi[8], Alex Archibald[6], Gufran Beig[3]

[1]Lancaster Environment Centre, Lancaster University, Lancaster, LA1 4YQ, UK
[2]Data Science Institute, Lancaster University, Lancaster, LA1 4YW, UK
[3]Indian Institute of Tropical Meteorology, Pune, India
[4]Environmental Science, Dept. of Botany, Utkal University, Bhubaneswar, India
[5]Centre for Atmospheric Sciences, School of Earth, Atmospheric and Environmental Sciences, University of Manchester, Manchester, UK
[6]NCAS-Climate, Department of Chemistry, University of Cambridge, Cambridge, UK
[7]National Atmospheric Research Laboratory, Gadanki, AP, India
[8]Centre for Atmospheric and Climate Physics Research, University of Hertfordshire, Hatfield, Hertfordshire, UK
[9]School of Mathematics, University of Manchester, Manchester, UK

Correspondence to: Ying Chen (y.chen65@lancaster.ac.uk)

Contents of this file

S1. Comparisons between observations and model results of domain-03 and domain-04

The model (driven by ECMWF) results of domain-03 (D03, 5 km) and domain-04 (D04, 1.67 km) are compared with observations, as shown in Fig. S98. One can see that the model performance is not improved with higher resolution in D04. The median and mean values of $PM_{2.5}$ and ozone from D03 simulation agree well with observations, although there is slightly overestimation of NOx. The $PM_{2.5}$ and NOx, which are mainly primary pollutants, are even more overestimated by D04 than by D03. The secondary pollutant ozone is therefore more underestimated by D04, due to depleted by too much NOx. These may imply an overestimation of NOx emission in the inventory and/or an underestimation of horizontal mixing efficiency in the WRF-Chem model with high resolution simulations.

S2. Comparison between simulations driven by ECMWF and NCEP datasets

The model performance of meteorology simulation is validated by the measurements in Delhi as shown in Fig. S109 (temperature-T and relative humidity-RH) and Fig. S110 (wind pattern). Both simulations driven by ECMWF and NCEP datasets reproduce the T very well with averaged factor around 1 and R=0.9 compared with measurements, although some underestimations can be found in the results driven by ECMWF when T is less than 35°C. The model results driven by ECMWF reproduce RH fairly well (R=0.7), and much better than the NCEP one (R=0.4). The model results driven by NCEP under-predict RH by 20-40%, despite an underestimation in high RH regime (RH>50%) can also be observed in the results driven by ECMWF. These findings are consistent with a recent study (Chatani and Sharma, 2018), which shows the WRF-Chem driven by ECMWF can reproduce much better meteorological conditions compared with observations over India than the driven by NCEP. They also reported that this is a general situation over the whole year (2010) of India and North Pakistan simulation, but the pre-monsoon (April-May) possibly experiences the largest underestimation of RH by

more than 20% over Delhi in the results driven by NCEP. The observed wind pattern, dominated by the West-North wind direction, is reasonably captured by simulations driven by both ECMWF and NCEP (Fig. S11~~0~~). Simulation driven by NCEP produces slightly better wind direction than the one driven by ECMWF, but with a slight overestimation of wind speed can be observed as indicated by less blue colour regions in Fig. S11~~0~~b.

The model driven by NCEP data predicts slightly lower $PM_{2.5}$ (Fig. S1-S2) and very close O_3 (Fig. S5-S6) concentrations compared to the ECMWF driven one, although a large difference in relative humidity can be found. The lower $PM_{2.5}$ values from NCEP driven results possibly due to the higher height of PBL, which can approach ~3500 meter during afternoon in contrast of ~2500 meter of the ECMWF driven one. The deeper PBL dilutes the fresh emitted $PM_{2.5}$ in the surface layer. This can be especially important in Delhi, where primary particles are the major contributor to $PM_{2.5}$ during pre-monsoon (see section 3.1), and secondary inorganic aerosol (SIA), including sulphate, nitrate and ammonium, only contributes 20-25% of $PM_{2.5}$ loading in both ECMWF and NCEP results. It is worth noting that the difference in relative humidity results between model driven by ECMWF and NCEP may have a larger impact on $PM_{2.5}$ loading and SIA formation during winter period in Delhi when the atmosphere is more humid.

In general, the model driven by ECMWF can produce better meteorological conditions and $PM_{2.5}$ results than the NCEP driven one, while similar O_3 results are found. In this study, our baseline simulation is driven by ECMWF dataset.

S3 Regional Influence of the Delhi Urban Plume

The pollution plume from local emissions in Delhi can also influence downwind regions, particularly to the southeast of Delhi in this season due to the prevailing northwest wind. Fig. S12~~1~~ shows the spatial distribution of SIs corresponding to traffic emissions for $PM_{2.5}$ and O_3 over Delhi and nearby regions. We consider only the local traffic sector (TRA) here, since it is the governing factor for both $PM_{2.5}$ and O_3 in Delhi, and the major contributor of primary $PM_{2.5}$ and NOx. In this study, we use O_3 peak hour (15:00 LT) with the fully developed PBL to represent the influence of plume in daytime. And we use the early morning before PBL development (05:00 LT) to represent the influence in night, which shows a strong regional interaction indicated by the highest sensitivity of $PM_{2.5}$ to the emissions from NCR emissions (Fig. 4a). In general, the Delhi urban plume has a broader influence at night, possibly facilitated by favourable meteorological conditions of strong regional interactions. The NOx-rich urban plume depletes O_3 in downwind regions during the night with sensitivity larger than 70%, in contrast of a negligible sensitivity (<10%) for $PM_{2.5}$. This indicates that Delhi urban plume has a larger and broader impact on O_3 than on $PM_{2.5}$ in the downwind regions.

Table S1. SAFAR network measurements in Delhi.

No.	Station Name	Short Name	Latitude	Longitude	$PM_{2.5}$	O_3	NOx	Meteorology	Environment Describe
1	C V Raman	CVR	28.72	77.20	Yes	--	--	--	Downtown
2	Delhi University	DEU	28.69	77.21	Yes	--	--	--	Highly populated Residential
3	Airport T3	AIR	28.56	77.10	--	Yes	Yes	--	Airport city side
4	Ayanagar	AYA	28.48	77.13	--	Yes	--	Yes	Suburban background
5	NCMRWF	NCM	28.62	77.36	--	Yes	--	Yes	Industrial, Upwind Entry
6	Pusa	PUS	28.64	77.17	--	--	--	Yes	Background

Table S2. Design of training runs for building Gaussian process emulator.

Training Runs No.	Factors for each emission sector			
	DOM (area source)	**TRA (line source)**	**POW+IND (point source)**	**NCR* (regional transport)**
1	1.2958	0.87408	1.0316	0.33741
2	0.75507	1.556	1.8606	0.45469
3	0.48991	0.95171	0.22896	1.416
4	1.4326	1.779	0.63716	1.3508
5	1.3191	0.40663	0.59954	1.1988
6	0.067129	0.023068	1.1011	0.50473
7	0.92064	1.83	0.19348	0.06012
8	0.1336	0.19012	0.38896	0.87948
9	0.37848	1.449	0.90053	1.0461
10	1.6056	0.51501	0.013731	0.75497
11	0.51618	1.2396	1.7039	1.208
12	1.12	0.62141	1.3866	0.96124
13	0.84394	0.20906	0.4144	1.8251
14	0.60487	0.3878	1.6648	1.7574
15	1.5254	1.991	1.4452	1.5008
16	1.784	1.629	0.87087	0.23874
17	1.8007	1.0225	1.2664	1.6046
18	1.0119	1.1866	1.5495	1.9241
19	0.26926	0.73029	0.79889	0.17177
20	1.9168	1.3829	1.9492	0.66879

**Emissions in the National Capital Region surrounding Delhi (domain-03 as shown in Fig. 1), representing the influence of regional transport from surrounding Delhi.*

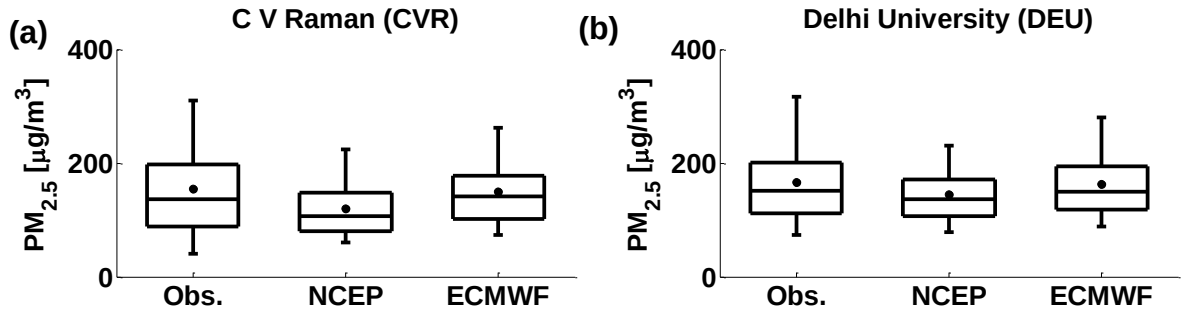

Figure S1. Comparison of the frequency distributions of observed and modelled (driven by NCEP and ECMWF datasets) hourly $PM_{2.5}$ concentrations. (**a**) CVR; (**b**) DEU. The boxplots show the median, mean (black dot), 25% percentile, 75% percentile, 95% percentile and 5% percentile values.

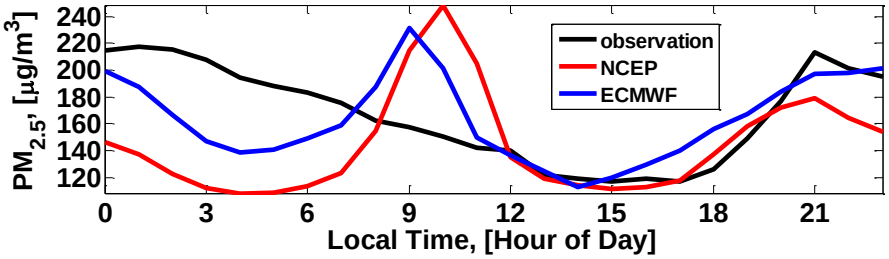

Figure S2. Diurnal patterns of $PM_{2.5}$ at DEU site (marked in Fig. 2). The results are averaged during 02-15 May 2015.

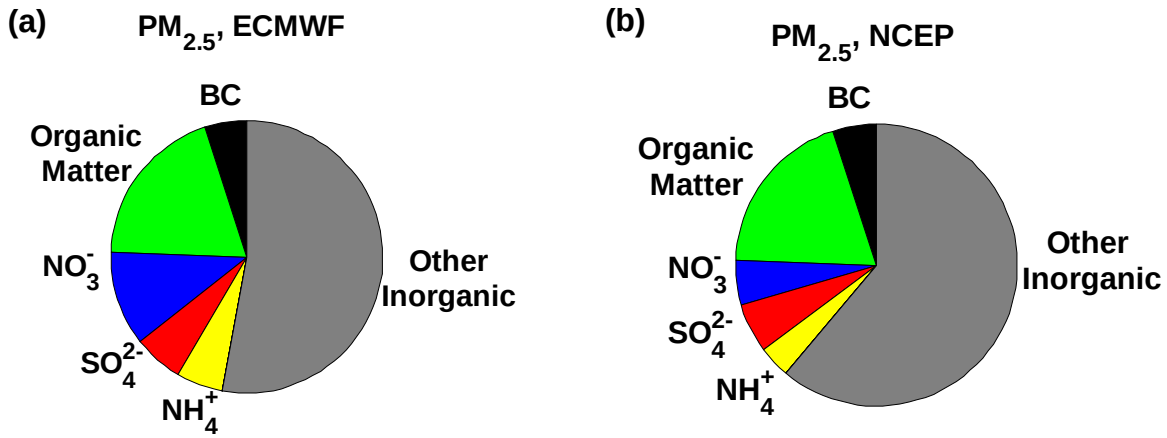

Figure S3. The simulated compositions of $PM_{2.5}$ at Delhi city background site (PUS). The modelled masses of each compounds are averaged during 02-15 May 2015. (**a**) drive by ECMWF data; (**b**) drive by NCEP data.

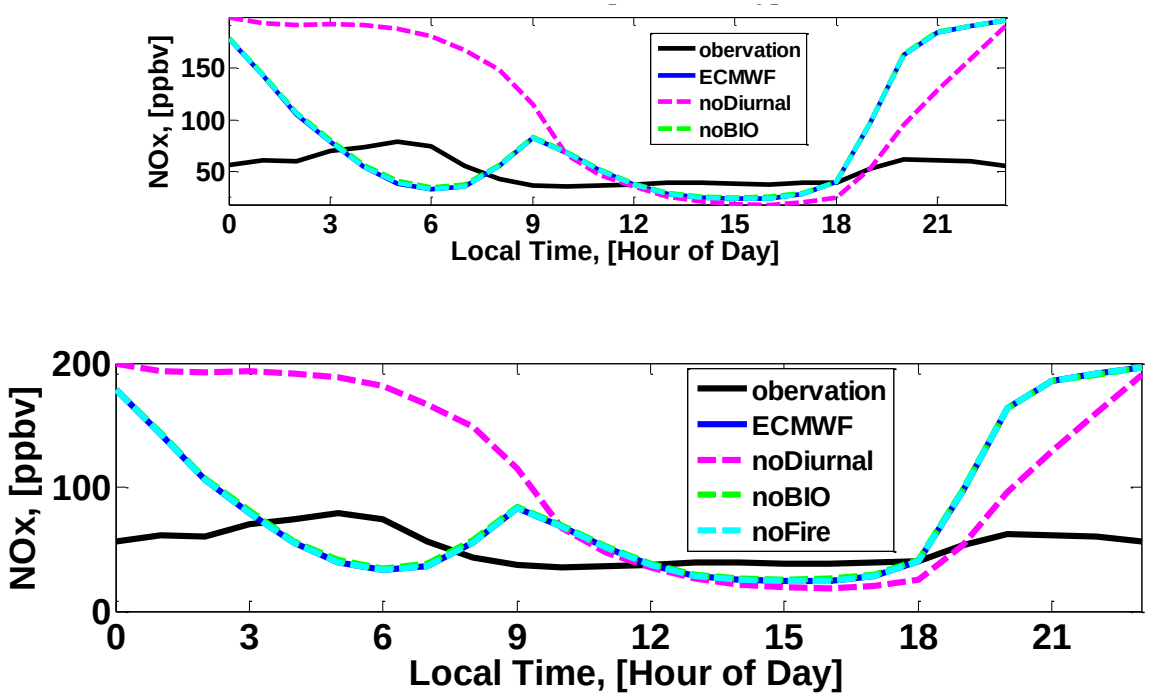

Figure S4. Diurnal patterns of NOx concentration from WRF-Chem model and observational results at AIR site (marked in Fig. 2). The results are averaged during 02-15 May 2015. Note that ~~'NCEP' and~~ 'ECMWF' indicates the model results driven by ~~NCEP and~~ ECMWF reanalysis data~~, respectively~~.

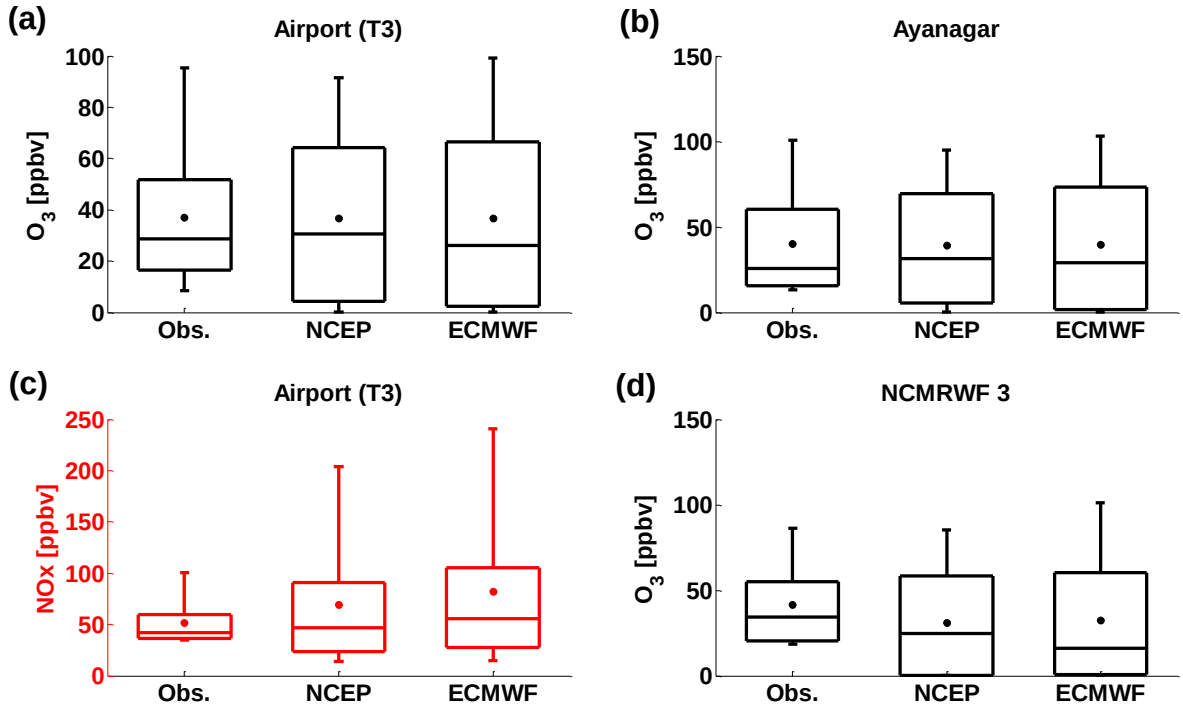

Figure S5. Comparison of the frequency distributions of observed and modelled hourly results (driven by NCEP and ECMWF datasets). (**a**) O_3 at AIR; (**b**) O_3 at AYA; (**c**) NOx at AIR; (**d**) O_3 at

NCM. The boxplots show the median, mean (black dot), 25% percentile, 75% percentile, 95% and 5% values.

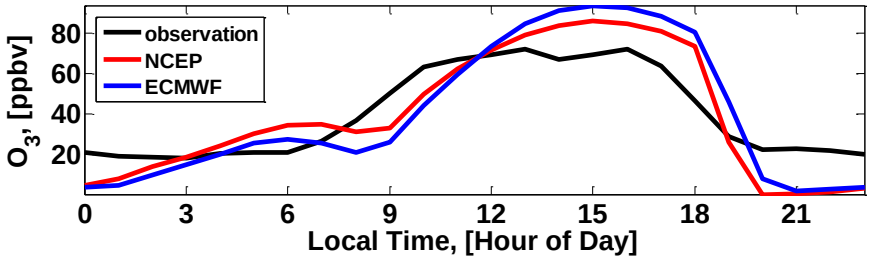

Figure S6. Diurnal patterns of O_3 at AYA, similar as Fig. S2. The 'NCEP' and 'ECMWF' indicate the model results driven by NCEP and ECMWF datasets, respectively.

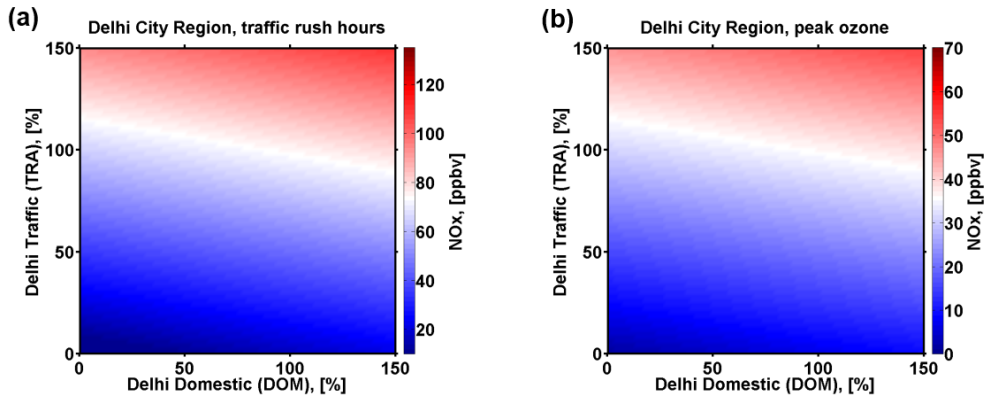

Figure S7. Response surfaces for NOx concentrations over Delhi City Region as a function of local traffic and domestic emissions in Delhi, during average rush hour (**a**) and ozone peak period (**b**).

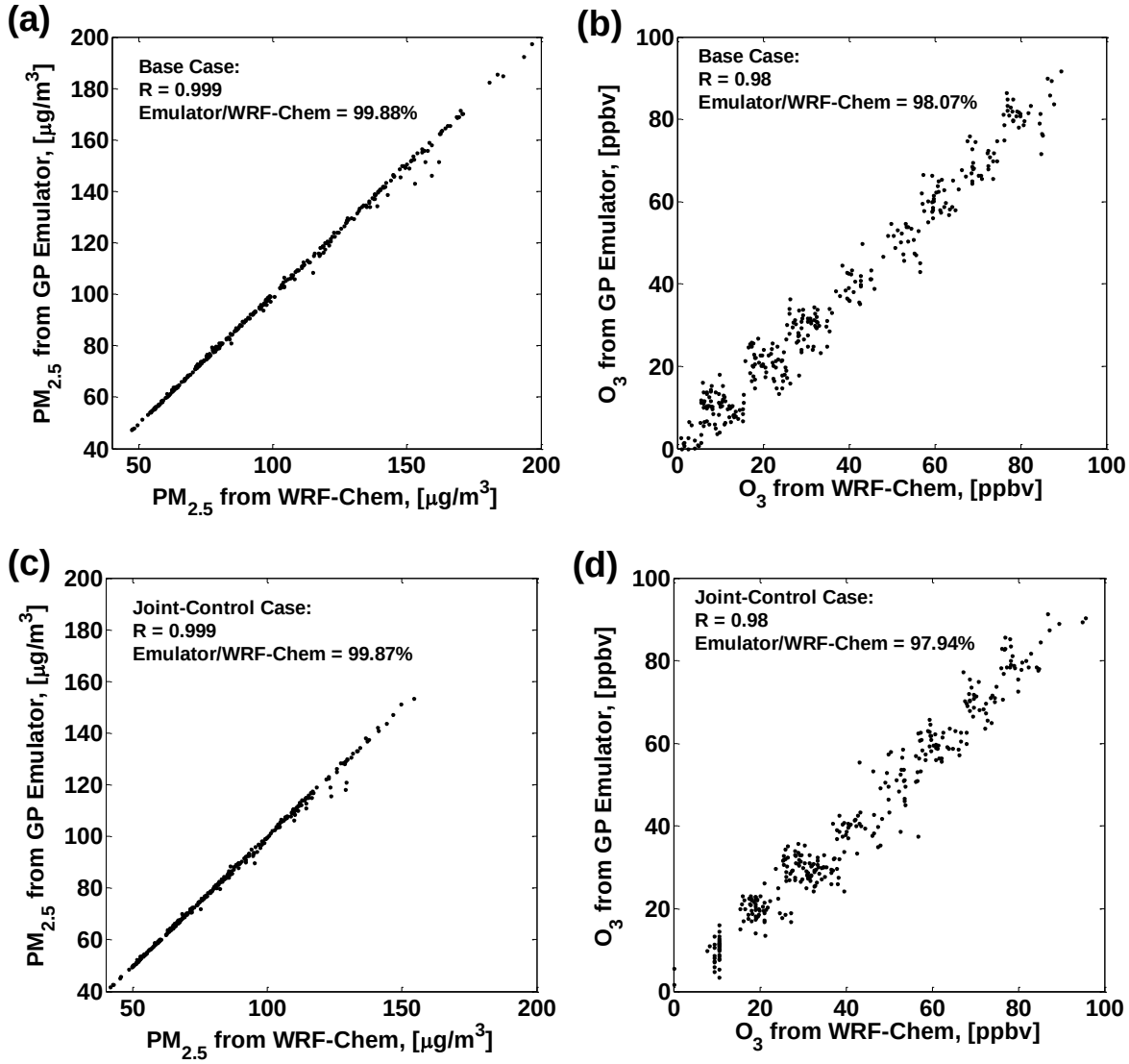

Figure S8. Extra validation of Gaussian process~~P~~ emulator results in the mitigation strategy according to Fig. 7. The accuracy of ~~GP~~the emulator for reproducing current conditions of $PM_{2.5}$ **(a)** and O_3 **(b)**, i.e. base case without changing emissions. The accuracy of ~~GP~~the emulator for reproducing regional joint coordination conditions of $PM_{2.5}$ **(c)** and O_3 **(d)**, i.e. NCR joint control case with local traffic emissions reduced by 50% and regional emissions reduced by 30%. All the results are averaged over Delhi City Region, with hourly resolution during the simulation period.

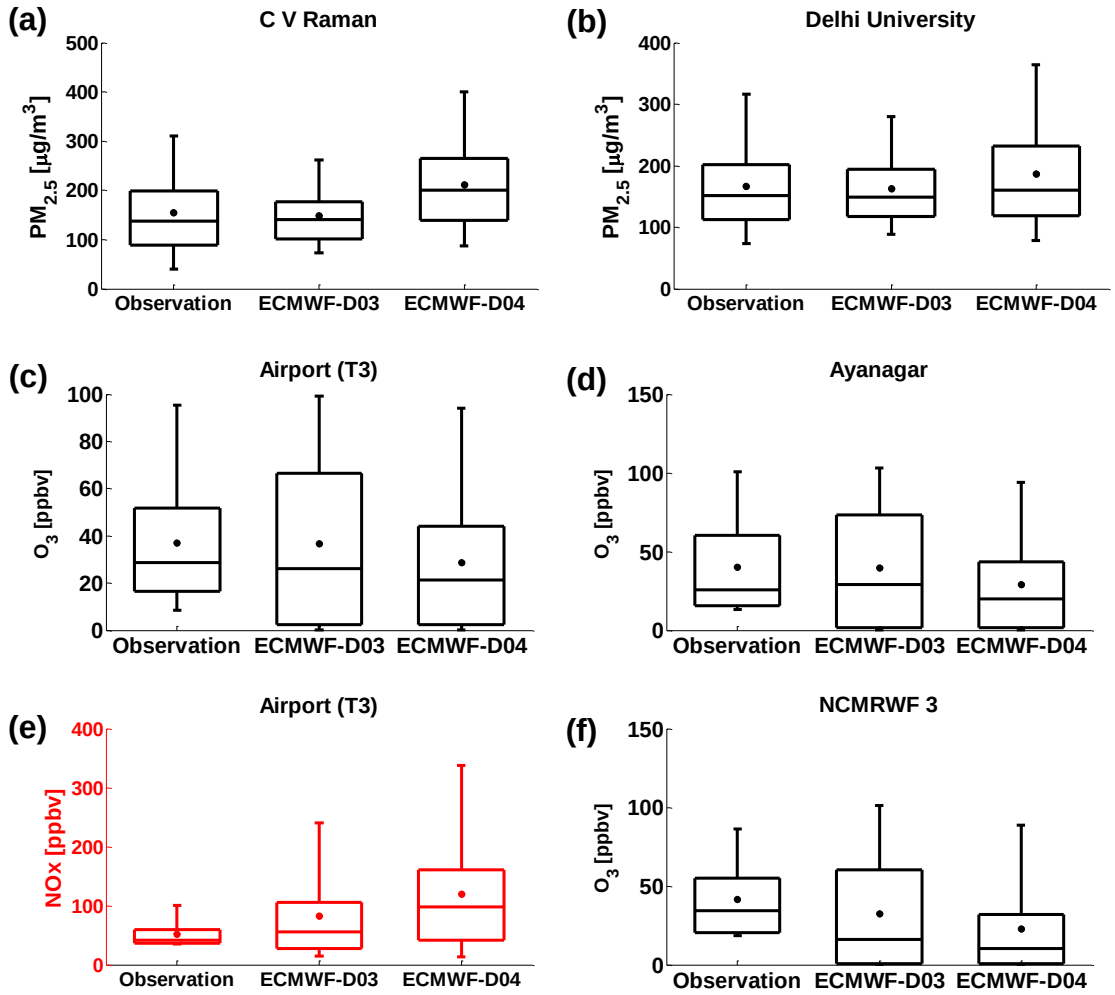

Figure S98. Comparisons of frequency distributions between observations and model results of domain-03 and domain-04. (**a**) $PM_{2.5}$ at CVR; (**b**) $PM_{2.5}$ at DEU; (**c**) O_3 at AIR; (**d**) O_3 at AYA; (**e**) NOx at AIR; (**f**) O_3 at NCM. The WRF-Chem model was driven by ECMWF dataset.

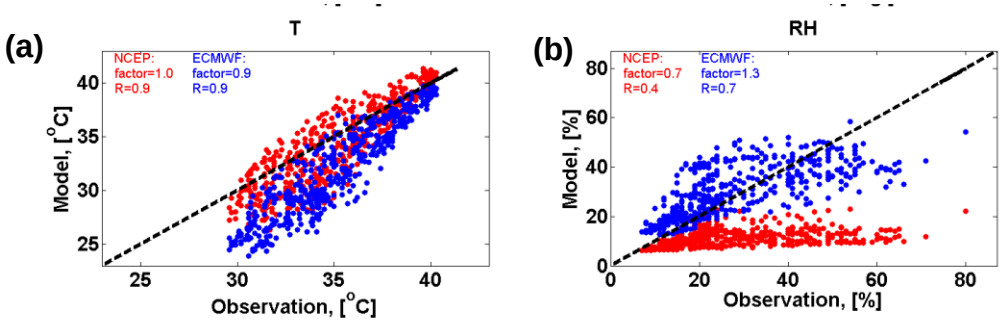

Figure S109. Comparisons of modelled meteorological conditions with all measurements over Delhi. (**a**) temperature (T); (**b**) RH. The red dots indicate the results of WRF-Chem driven by NCEP reanalysis data, blue dots indicate the results of WRF-Chem driven by ECMWF reanalysis data, and the black dashed line indicates the 1:1 line. The measurement sites are given in Table S1, and the corresponding model results are extracted.

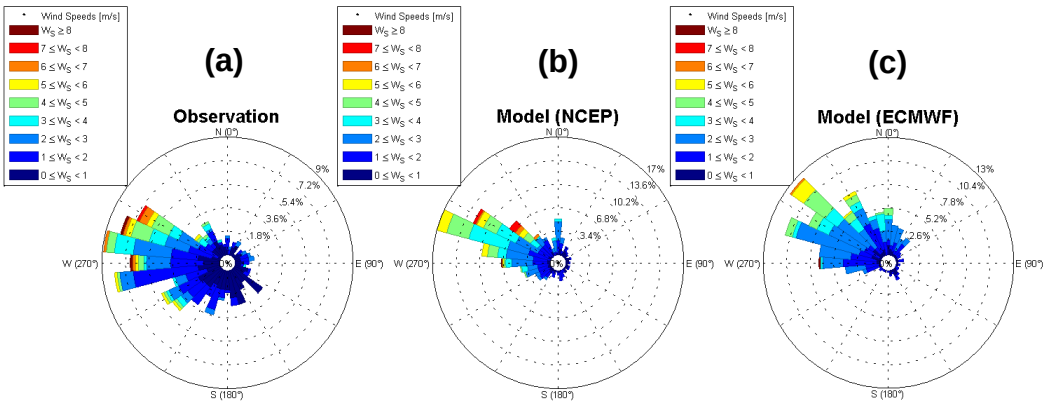

Figure S1~~0~~. Wind rose pattern of measurements and modelled wind pattern over Delhi. The results from all sites are shown. (**a**) observations; (**b**) model driven by NCEP; (**c**) model driven by ECMWF. The measurement sites are given in Table S1, and the corresponding model results are extracted.

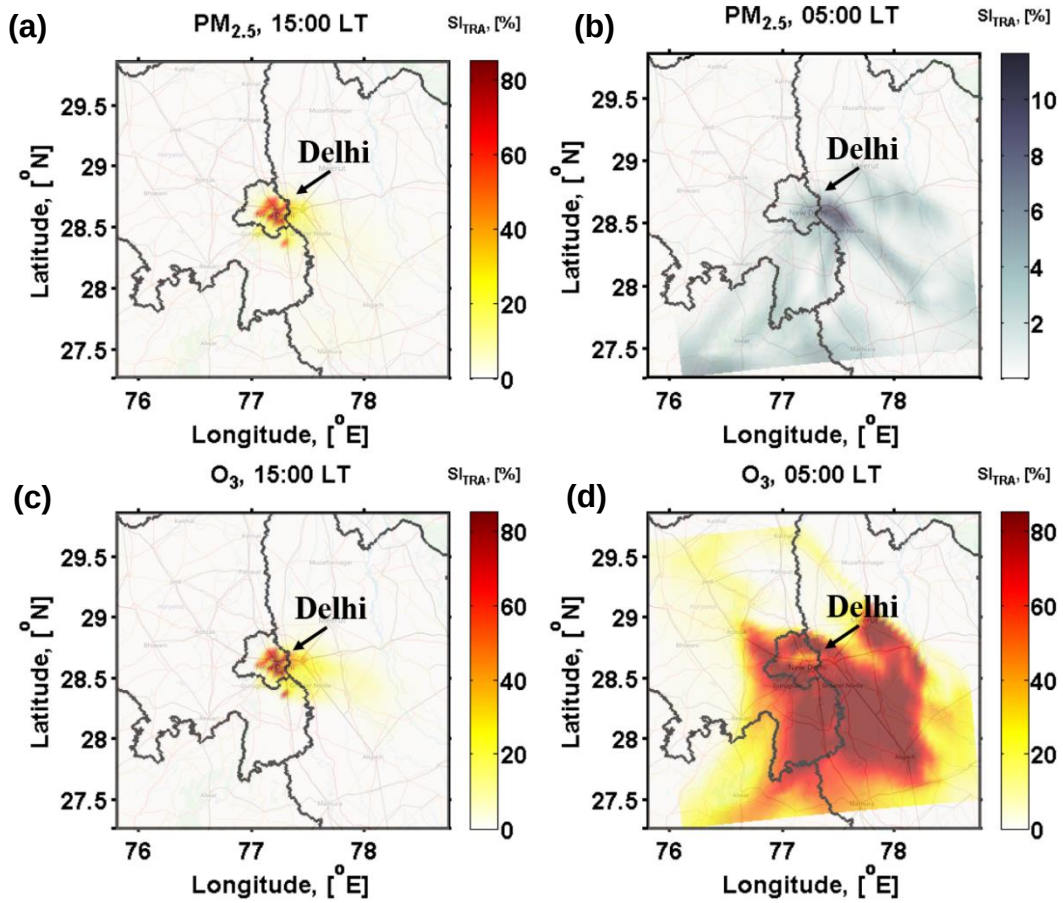

Figure S1~~1~~. Horizontal distribution of sensitivity index for local traffic emissions in Delhi (SI_{TRA}). The model results are averaged over 02-15 May 2015. Sensitivity indices are shown for: (**a**) $PM_{2.5}$ during ozone peak hour (15:00 LT), (**b**) $PM_{2.5}$ before PBL developed (05:00 LT), (**c**) O_3 at 15:00 LT, and (**d**) O_3 at 05:00 LT. Noting that the scale of colorbar in panel (b) is different from the others.

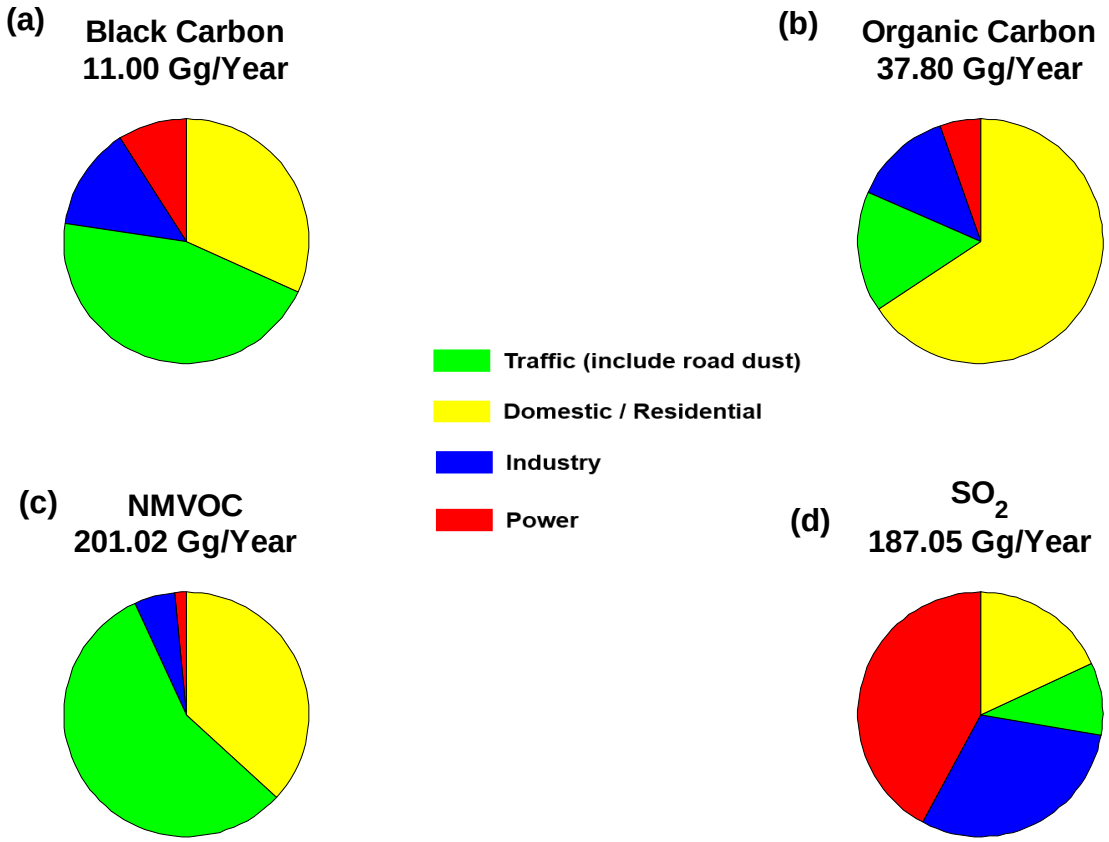

Figure S13~~2~~. Annual emission of different sectors in Delhi from SAFAR inventory. (a) black carbon; (b) organic carbon; (c) non-methane VOC and (d) SO_2.

Supplementary References:

Chatani, S., and Sharma, S.: Uncertainties Caused by Major Meteorological Analysis Data Sets in Simulating Air Quality Over India, Journal of Geophysical Research: Atmospheres, 123, 6230-6247, doi:10.1029/2017JD027502, 2018.